Conceptual Fuselage Design with Direct CAD Modeling

by

Benjamin K. Anderson

A Thesis Presented in Partial Fulfillment
of the Requirements for the Degree
Master of Science

Approved April 2017 by the
Graduate Supervisory Committee:

Timothy Takahashi, Chair
Jay Patel
Akif Bolukbasi

ARIZONA STATE UNIVERSITY

May 2017

ABSTRACT

In today's day and age, the use of automated technology is becoming increasingly prevalent. Throughout the aerospace industry, we see the use of automated systems in manufacturing, testing, and, progressively, in design. This thesis focuses on the idea of automated structural design that can be directly coupled with parametric Computer-Aided Drafting (CAD) and used to support aircraft conceptual design. This idea has been around for many years; however, with the advancement of CAD technology, it is becoming more realistic. Having the ability to input design parameters, analyze the structure, and produce a basic CAD model not only saves time in the design process but provides an excellent platform to communicate ideas. The user has the ability to change parameters and quickly determine the effect on the structure. Coupling this idea with automated parametric CAD provides visual verification and a platform to export into Finite Element Analysis (FEA) for further verification.

This Thesis is dedicated to my family, whose love and support made my education possible. To my Mom and Dad, I could not have done this without your unwavering support. Thank you for listening and being there every step of the way. Words cannot express how thankful I am for everything you have done. To Matt and Jocelyn, thank you for being my best friends, for the care packages, and bringing laughter and joy when I needed it most.

ACKNOWLEDGMENTS

Special thanks to Dr. Raghavendra Murthy for taking the time out of his busy schedule to answer my many ANSYS questions, and to my supervisory committee for taking the time off work and out of their day to attend my defense.

TABLE OF CONTENTS

Page

Page

APPENDIX Page

LIST OF TABLES

Table Page

Table Page

LIST OF FIGURES

Figure Page

Figure Page

Figure Page

NOMENCLATURE

Alt = Altitude (ft)

A = Area (in^2)

A_s = Cross-Sectional Area (in^2)

$\bar{c}$ = Mean Geometric Chord (ft)

CL = Coefficient of Lift

DR = Design Range (Nm)

E = Young's Modulus (lbf/in^2)

P_c = Compressive Force (lbf)

P_s = Shear Force (lbf)

F_{tu} = Material Ultimate Strength (lbf/in^2)

F_{ty} = Material Yield Strength (lbf/in^2)

I = Area Moment of Inertia (in^4)

K_c = Compressive Buckling Coefficient

K_e = Fixtivity Constant

Ks = Shear Buckling Coefficient

L = Length (in)

l = Tail Moment Arm (ft)

M = Fuselage Bending Moment (lbf-in)

N_z = Load Factor (g)

OEW = Operational Empty Weight (lbm)

$\bar{P}$ = Pressure (lbf/in^2)

ΔP = Pressure Differential (lbf/in^2)

q = Dynamic Pressure (lbf/in^2)

$\bar{q}$ = Shear Flow (lbf/in^2)

r = Radius (in)

S_{HT} = Horizontal Tail Surface Area (ft^2)

Sref = Wing Reference Area

S_{VT} = Vertical Tail Surface Area (ft^2)

t = Thickness (in)

V_C = Cruise Speed (KIAS)

V_D = Dive Speed (KIAS)

W = Weight (lbm)

y = Distance from Neutral Axis (in)

ρ = Radius of Gyration

μ = Poisson's Ratio

Λ = Sweep Angle (radians)

INTRODUCTION

The conceptual design phase is the starting point for any airframe development program. It is during this phase that engineers brainstorm large scale design concepts. This results in a fluid design; however, it is difficult to develop a detailed Computer-Aided Drafting (CAD) model. In many instances, a quick "napkin sketch" is made to communicate an idea. Depending on the artistic ability of the designer, this may not be an effective approach. As technology improves, the idea of automated CAD is more realistic, allowing engineers to enter various parameters and rapidly model ideas. Something of this nature not only improves communication, but drastically improves the efficiency of the conceptual design team. Time is money in the aerospace industry and anything that can decrease the time between idea conception and product delivery should be explored.

While the conceptual design phase is by no means an area for detailed CAD modeling, a somewhat accurate depiction of the geometry under investigation is of great use for a design team. This model serves as a platform to provide preliminary weight estimates, structural integrity, and enables designers to handpick features. In an advanced model, the designer could add or remove windows and exits, or change the cabin pressure, and see how the basic airframe structure reacts. This is especially useful when working alongside a marketing team which may inquire about additional windows or lower cabin pressure. This type of tool could enable the engineer to rapidly change the design and provide immediate feedback on the design impact.

Embedding a detailed structural sizing tool into a CAD program and rapidly modeling up conceptual ideas not only allows for easier communication, but also

provides an excellent platform when the program moves into detailed design. By modeling the structure in a CAD program and exporting this representation to Finite Element Analysis (FEA), the designer can identify stress "hot spots" and other potential sources of weakness or weight growth within the conceptual design (see Figure 1). While further structural analysis will surely be warranted later in the preliminary design, it is useful to identify potential issues as early on in the design as possible. The author acknowledges that it is nearly impossible to accurately predict the structural integrity of the final design, but instead suggests a tool of this nature will provide valuable insight going into the detailed design phase.

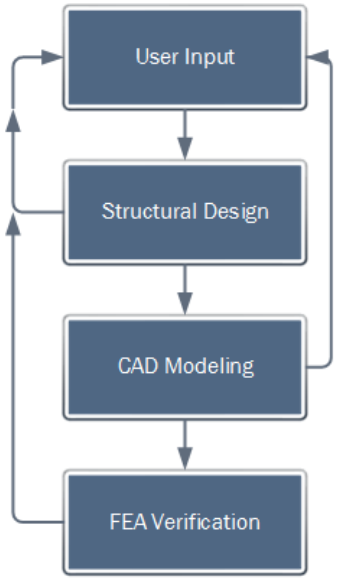

Figure 1. Design Process

PRIOR ART

Industry and Government Development

The idea behind rapidly producing aircraft sketches is nothing new. Many programs have been developed over the years in an attempt to streamline the conceptual design phase.

An early attempt at automated conceptual design came from Dr. Richard H. MacNeal of the Lockheed Aircraft Corporation in 1956. In his paper titled, "Automatic Structural Design Optimization" [1] MacNeal outlines his approach at an automated structural design method. This approach iterates through design geometry until a light weight configuration meeting all structural design requirements is found. The process involves selecting structural geometry and then optimizing the geometry based on applied loads. Due to the timing of his paper, many of the design processes were still under development including integrally stiffened panel analysis which he states was "at best a year away."[1] While MacNeal's objectives were largely similar to the goals of the present paper, MacNeal was limited by the technology of his time. MacNeal would later go on to co-found the MacNeal-Schwendler Corporation (MSC) which developed the first structural analysis software called Structural Analysis by Digital Simulation of Analog Methods (SADSAM).[2] This program was the basis for the analysis software NASTRAN which is still in use throughout the aerospace industry.[2]

Around the same time as MacNeal, Lucien A. Schmit, Jr. was working on similar structural design analysis methods as outlined in his 1960 paper "Structural Design by Systematic Synthesis"[3] Schmit's main focus was the idea of design cycle automation and optimization. At this time the use of computers was rapidly improving design

methods and enabling the use of previously impractical approaches. Schmit describes the design cycle in three phases: "1. Establish a trial design; 2. Carry out an analysis based on the trial design; 3. Based on the analysis, modify the trial design."[3] He then constrains his design with requirements such as design load, stress and deflection limits, and overall sizing limitations.[3] By effectively developing a program that performs these tasks, Schmit was able to design what he refers to as "elementary examples" involving a three beamed truss.[3] While Schmit's work was also limited by the technology of the time, it provided a basis for future structural design work, and is still widely applicable to present design methodology.

Garret Vanderplaats, who was Schmit's PhD student at Case Western Reserve University, furthered the work of design optimization. In his paper titled "Automated Optimization Techniques for Aircraft Synthesis," Vanderplaats discusses his use of Multi-Disciplinary Design (MDD) and Multi-Disciplinary Optimization (MDO) to size aircraft subject to certain design objectives, variables, and constraints.[4]

Vanderplaats later developed complex FEM based structural optimization methods marketing his code commercially as a product known as GENESIS. He, along with his colleagues Rastogi and Ghosh, discuss some of GENESIS's optimization capabilities in their paper titled "Discrete Optimization Capabilities in GENESIS Structural Analysis and Optimization Software."[5] His company, Vanderplaats Research and Development, has developed software capable of solving very large-scale optimization problems with hundreds of thousands of design variables. At the time of publication (2002), their design program BIGDOT was capable of solving a continuous optimization problem with a hundred-thousand variables, which has surely increased in

the past decade.[5] Their paper also discusses composite lay-up optimization which can be used to determine the best ply orientation in composite structures. As composites grow in popularity due to their high strength, low weight characteristics, this feature will be of significant importance in the present design world. While the present paper does not focus on the use of MDD or MDO methods, it is impressive to note the design optimization capability created from Vanderplaats' work.

Following in the footsteps of MacNeal, and Vanderplaats, Lockheed Martin continues to develop innovative tools and processes to aid in their aircraft development programs. In 2002, Atherton Carty of the Lockheed Martin Aeronautics Company discusses what he calls a Rapid Conceptual Design (RCD) methodology in his paper titled "An Approach to Multidisciplinary Design, Analysis & Optimization for Rapid Conceptual Design."[6] This methodology is centered on rapid conceptual design through the use of MDD and MDO across all design areas.[6] The RCD software conducts automated studies and optimizations enabling quick changes across all systems whenever a design change occurs. Through this study he found the use of automated parametric design tools greatly reduced the time necessary to evaluate design changes.

Expanding further on the RCD methodology, Carty & Davies began to integrate parametric CAD as outlined in their 2004 AIAA paper titled, "Fusion of Aircraft Synthesis and Computer Aided Design."[7] While the process outlined in this paper is far beyond the scope of the present paper, the concepts employed by Carty and his team are very much applicable. Carty discusses how the integration of a CAD model into their RCD methodology has provided accurate feedback on design parameter changes taking place within their program. They also discuss the benefits of having a CAD model when

it comes to updating vortex-lattice geometries and the ability to generate mesh models for FEM and CFD analysis. While the present paper will not focus on MDD or MDO, it is useful to note the success and time savings others have found with the use of parametric design tools.

One subject pointed out in both of Carty's papers [6] [7] is the challenge related to updating legacy codes throughout the industry. As design concepts change, these programs often have to be updated to handle new innovative ideas. In a perfect world these programs could be designed to handle anything, however, it is nearly impossible to anticipate what the future holds. While this problem is inevitable, great care has been taken to ensure the tool discussed in the present paper is as flexible as possible.

Continuing on the trend of large aerospace companies and their usage of automatic parametric CAD leads us to Jan H. Vandenbrande and his colleagues at The Boeing Company. In their paper titled, "The Search for the Perfect Body; Shape Control for Multidisciplinary Design Optimization,"[8] the authors discuss the use of an optimization tool with the usage of what they call the General Geometry Generator (GGG). This program takes user input and generates the desired geometry. The authors go in depth on the process behind generating models automatically in a CAD program. This process includes writing code to control splines, surfaces, and sections to generate the model through lofts. They also point out many nuances inherent to CAD parametrization including broken constraints, shape control, code generation, and discontinuity within line elements.

Around the same time frame, Christof Ledermann created a tool outlined in his 2006 paper titled, "Dynamic CAD objects for structural optimization in preliminary

aircraft design."[9] This program is designed to take structural design optimization into account and directly model the structure in CATIA V5. Unlike similar programs, Ledermann's tool takes into account the entire airframe instead of simply focusing on the wing or fuselage. While this paper discusses internal structure, its main focus lies in CAD integration. The author simplified the overall structural analysis by limiting the optimization to one load case and only featuring simple buckling analysis. The goal of this thesis is to expand on the work of Ledermann and develop a tool that takes into account multiple structural loading cases, as well as buckling, before developing a direct CAD model.

The National Aeronautics and Space Administration (NASA) has also been a big proponent of automated conceptual design technology. Starting in the early 1990's, NASA/Langley began development of an integrated CAD design tool called FIDO (Framework for Interdisciplinary Design Optimization), which was found to be troublesome due to the maturity of CAD programs at that time.[9] Around the 2010 time frame, NASA/Langley developed another conceptual design tool known as Vehicle Sketch Pad (VSP).[10] [11] Unlike similar programs, the decision was made early on in the program development to cut commercial CAD entirely out of the process. This decision was made because it was deemed too expensive and would require a skilled CAD operator to remain on their staff. They instead developed their own parametrized modeler which was easy to learn and produced detailed sketches based on a user's inputs. This basic model was used by the Nasa/Langley engineers to create vortex-lattice models and support rapid prototyping. While VSP does offer some internal structural layout capability, its primary focus is on external geometry and aerodynamic analysis.

NASA/Langley is also responsible for what is now known as HyperSizer, a well-known structural design suite.[12] Beginning in 1988, a team at the NASA/Langley research center started developing software known as ST-SIZE to aid in the development of new high speed aircraft.[12] According to Craig Collier, one of the engineers responsible for ST-SIZE, "Its purpose was to do a very fast weight-reduction using different design concepts and configurations of vehicles…"[12] Through the technology transfer program, Collier obtained a licensed version of ST-SIZE and created what is now known as HyperSizer. This program is used at industry giants such as Lockheed Martin, The Boeing Company, and Northrop Grumman to aid in the structural development of future aircraft; it is also currently being used at NASA to help with the development of the Orion Spacecraft.[13] According to the HyperSizer website, the current version "performs design, stress analysis, and detail sizing optimization for aircraft and space launch vehicles… HyperSizer replaces the need for spreadsheets and 'hand calculations'…"[13]

Recent Progress throughout Academia

While there have been many attempts at automated conceptual design technology throughout the aerospace industry, there have also been great strides within academia. In 2003, Juan Alonso of Stanford University led a team of engineers in designing a structural design tool utilizing parametric CAD technology. In their paper titled, "High-Fidelity Aero-Structural Design Using a Parametric CAD-Based Model,"[14] the authors outline their process of automated structural design and parametric CAD modelling. They also discuss the development of a tool which analyzes both structural integrity and

aerodynamic flow. Utilizing a program they call AEROSURF the authors create a parametric CAD model of their conceptual design. This model includes the fuselage, wing, vertical and horizontal tails, and engine nacelles.[14] After creating the AEROSURF models the authors use CFD and finite element software they call FEAP to analyze their design. The focus of this work, similar to the NASA VSP program, is on the aerodynamic geometry and wing structure, while the internal fuselage structure is not mentioned.

Similar to the work conducted by Alonso, and his team, a paper written by a group of engineers at the University of Arizona outlines an attempt at designing fully parametrized wing models. The paper, by Hutchins, Missoum & Takahashi titled, "Fully Parametrized Wing Model for Preliminary Design" [15] discusses how to design and optimize wing structure using ANSYS and VORLAX. The authors utilize ANSYS to create a "highly parametrized" finite element model, along with VORLAX to analyze the stress, pressure loads, and natural frequencies present in a proposed wing structure.[15]

Another paper written by Lemonds & Takahashi outlines a tool developed at Arizona State to analyze wing structure and direct CAD integration. The paper titled "Prediction of Wing Structural Mass of Transport Category Aircraft Conceptual Design"[16] discusses the development of a semi-empirical program designed to calculate the wing structural weight in transport category aircraft. The tool is designed to handle different wing geometries and analyze the structural qualities. Something particularly interesting about this tool is its ability to output wing geometry into a CAD model enabling further FEA analysis. This paper provided the basis to expand into internal fuselage structural design and develop a conceptual fuselage design tool coupled with direct CAD modeling which is the subject of the present paper.

After reading through numerous design papers focused on parametric CAD and conceptual aircraft design, the author noticed a significant lack of focus on internal fuselage structural design. The vast majority of these papers focus on the external geometry as it pertains to the aerodynamic characteristics of the aircraft, as well as internal wing structure. Attempts at internal fuselage design have been made, but many lack a focus on local panel buckling which results in inadequate structure. It is for this reason the present paper attempts to fill this void with a robust structural analysis tool coupled with a commercially available CAD program in an attempt to further explore the possibility of rapid conceptual fuselage design. These papers have, however, provided excellent insight into previous work and inspiration moving forward.

SUMMARY OF UNDERLYING STRUCTURAL ANALYSIS PRINCIPLES

Before any modeling can occur, a robust structural design algorithm is formulated to size structural elements and determine basic dimensions necessary for the CAD model. This is accomplished by first developing an analysis tool for the basic skin, stringer, and frame geometry, ignoring the various cutouts, bulkheads, etc. necessary for a full fuselage structure. The rationale behind this is to ensure the basic framework of the program is developed and functioning before tackling the more complex problems associated with cutouts and other structural elements.

Instead of following in the footsteps of some of the previous design tools utilizing globally iterative FEM solutions, this tool is built on the idea of direct rule-based synthesis. This decision was made due to the somewhat inaccurate nature of FEM solutions when it comes to analyzing compressive yield; although they correctly compute stress, many codes lack any form of buckling analysis. Aerospace structures are historically dominated by buckling concerns making the FEM based solutions inadequate. Instead of going down the non-linear FEM route, a rule-based synthesis method employing curved stiffened panel analysis and calibrated "crippling factors," similar to the work performed by Takahashi & Lemonds,[16] is used to obtain a decent first cut design.

The structural analysis tool requires a number of inputs before it can begin. These inputs include: aerodynamic loads, inertial flight loads, inertial ground loads due to a hard landing, cabin and flight altitude, lumped masses, a structural weight estimate, and the basic geometry (length, diameter, number of stringers, and desired frame spacing). These values are used to calculate the minimal structural requirements. Next, the

underlying code runs through automated hand calculations to determine if the desired geometry is feasible. These hand calculations are based off of equations presented in Michael Niu's *Airframe Structural Design* textbook [17] [18] in addition to well-known structural equations for column, panel, and stringer buckling.

Using the user inputs, the code analyzes the stringer and frame geometry to determine if the desired skin thickness, number of stringers, and frame spacing are feasible given the applied loads. This is done by calculating the stress present in each component and comparing it to the tensile yield and ultimate strength properties presented in MIL-HDBK-5J.[19] These limit loads are subject to a 1.5 factor of safety (FOS) as laid out in Title 14 of the Code of Federal Regulations (CFR) § 25.303.[20] Ultimately the tool analyzes the tensile and compression yield, local panel buckling present in curved panels, stringer buckling and crippling, and ultimate structural collapse. If the design is found to be infeasible the user is prompted to either reduce the applied loads or adjust the desired geometry.

Another important regulation pertinent to the design tool is 14 CFR § 25.305 (b)[21] which states,

> "When analytical methods are used to show compliance with the ultimate load strength requirements, it must be show that (1) The effects of deformation are not significant; (2) The deformations involved are fully accounted for in the analysis: or (3) The methods and assumptions used are sufficient to cover the effects of these deformations."

In other words, the skin of the aircraft is allowed to buckle under ultimate loads, but not limits loads. Proof must be provided that the aircraft is structurally sound. This can be shown either through load testing or non-linear FEM modeling of the buckled shape at the ultimate load. Neither of these methods are employed in this analysis, so the design tool is designed to prevent buckling in the skins under limits loads and the stringers under ultimate loads.

When it comes to structural aircraft design there are many different approaches to the same conclusion. In industry, every company develops their own design practices and most publish their own handbooks. Every design handbook differs slightly from the next and it is up to the design engineer to choose their own path. The primary reference handbook used for this thesis is *Airframe Structural Design*, by Michael Niu.[17] [18] This textbook draws heavily from Lockheed's design handbook used in the late twentieth century.

The primary focus of this design tool is to provide design assistance for fuselage skin thickness, stringer, and frame sizing. Following the input of the desired design features and loads, the tool analyzes the design feasibility and identifies potential shortfalls within the structure. These recommendations are based off an in depth structural analysis which takes into account tensile stresses, shear stresses, hoop stresses, compression yield stresses, local compression buckling of unsupported curvilinear panels, and global compression buckling of stiffened curvilinear panels. These considerations are based upon user specified loads including cabin pressurization, inertial loads, longitudinal flight loads, maneuvering loads, and ground loads. Finally, each design consideration is calculated and analyzed within the underlying structural analysis

code and output in a logical fashion making the feasibility of the desired structure clear to the user.

Materials Characterization

The material used for each component is specified within the input deck from a library of commonly used aerospace materials. These materials, such as Aluminum 2024-T3 and Aluminum 7075-T6, have been extensively researched by the United States Department of Defense. A full handbook of material properties has been published in the MIL-HDBK-5J titled, "Metallic Materials and Elements for Aerospace Vehicle Structures."[19] From this handbook, critical material properties including Young's Modulus, Poisson's Ratio, compressive ultimate and yield stress, and shear ultimate and yield stress are gathered and tabulated within the underlying code. These properties provide the ultimate structural limits for which the design must meet.

Within MIL-HDBK-5J,[19] the stress properties are divided into three categories: A, B and S. The A-basis is the value above which 99 percent of specimens will fail with a confidence of 95 percent. The B-basis is the value above which at least 90 percent of specimens will fail with a confidence of 95 percent. Finally, the S-basis is the minimum value as specified by federal or military standards.[19] According to 14 CFR § 25.613 (b),[22]

> "Material design values must be chosen to minimize the probability of structural failures due to material variability…the failure of which would result in loss of

structural integrity of the component, 99 percent probability with 95 percent confidence."

In other words, per the CFR, the minimum value (A or S basis) must be used as the design values. 14 CFR § 25.303 [20] also requires the material to be de-rated by a factor of 1.5, which is applied within the material library of this program. In an attempt to produce an optimized design compliant with federal regulations, these CFR regulations are accounted for and applied to the material properties used for the analysis. A worked example for the tensile yield strength of Aluminum 2024-T3 can be seen in Table 1.

Table 1. Example Design Stress with FOS

MIL-HDBK-5J Value (Fty)	42,000-lbf/in^2
Applied FOS.	1.5
Design Stress Limit	28,000-lbf/in^2

Another important material characteristic is the minimum gauge thickness. In many of the analytical solutions, such as skin thickness derived from hoop stresses, the results call for a material thickness far below what is seen in modern aircraft. This result was puzzling at first, but as the project progressed the reasoning behind the minimum gauge thickness became more apparent. According to the *FAA Handbook on Aviation Maintenance,* [23] the minimum gauge thickness is driven by fastener requirements. Larger commercial aircraft are not necessarily in this category, as their material characteristics are typically strength driven, but smaller general aviation aircraft are often oversized in the strength regime. For example, the minimum skin thickness for general aviation aircraft is typically 20 gauge (0.032-in) aluminum because the smallest available fastener is 3/32-in. While the use of adhesives would likely solve this issue, traditional fasteners

are still considered the norm. Therefore, the decision was made to limit material thickness to a minimum of 0.032-in within the design tool.

Similar to the minimum gauge skin thickness, the frame and stringer sizing is also set to a prescribed minimum. Again, this is done to ensure the airframe manufacturability. To allow for adequate space for the stringers, as well as future systems, the frame web height is limited to a minimum of two inches. This was determined after extensive analysis of the stringer sizing, which are set to have a minimum web height of half an inch. This minimum stringer height is typically seen along the sides of the fuselage where compressive stress is minimized. The upper and lower stringers, on the other hand, are typically much taller, requiring the minimum frame height of two inches. Again, this minimum is typically only seen in the smaller general aviation structures as the larger aircraft require more robust structure due to strength based requirements. A summary of all material requirements can be seen in Table 2.

Table 2. Summary of Requirements

Source	Requirement
14 CFR § 25.303 [20]	Applied 1.5 FOS
14 CFR § 25.305 [21]	No buckling at limit load
14 CFR § 25.613 (b)[22]	Must use minimum strength value (A or S Basis)
FAA Handbook on Aviation Maintenance[23]	Skin thickness may not be less than 20 gauge aluminum or 0.032-in thick.
Derived Requirement	Frame web may not be less than 2-in
Derived Requirement	Stringer web may not be less than 0.5-in

Structural Analysis – Shear and Moment Calculations

To determine the shear and compression loads on the airframe, the program calculates a shear and moment build up for the front and aft fuselage. The airframe is split in this manner due to the issue of where to "grab" the fuselage. In flight, the airframe is supported by the wings, and therefore, the loads are generally highest at the wing spar. Unfortunately, it is difficult to simulate the flight loads and resulting forces of flight without actually taking the aircraft up. This is simply not possible for new aircraft as it puts human life in danger. Therefore, the structure must be tested on the ground with simulated forces. To simulate this characteristic in a static structural test the airframe is fixed by the wing spar (see Figure 2). This divides the fuselage into forward and aft sections resulting in the maximum moment and shear loads occurring at the wing spar.

Figure 2. Example Structural Load Test. (2017, March 21). Retrieved from http://www.oneaircraft.com/static-testing-finished/

This method is a simplification to the actual loads developed in flight. When an aircraft flies, its inertial loads from gravity as well as rolling, pitching and yawing combine with aerodynamic loads. When trimmed, the aircraft balances upon its center of

gravity (CG) location where inertial forces counteract aerodynamic forces. When the aircraft pitches, the imbalance between aerodynamic and inertial forces drives its angular acceleration. Application of these real forces will eliminate any shear or moment discontinuity across the spar. Unfortunately, these loads are nearly impossible to duplicate in ground test. One could conceivably define an equivalent static load set to approximate the dynamic flight loads. However, this process is not implemented in this thesis work.

To create a shear and moment build up, the raw weight and applied forces are tabulated for every inch of the airframe starting at the nose and moving to the tail. The raw weight is calculated from a combination of point masses and distributed structural weight. The user supplies an estimated structural weight which is evenly distributed across the length of the airframe. Point masses are also supplied by the user and include components such as avionics, landing gear, payload, passenger furnishings, lavatories, auxiliary power unit (APU), etc. These components act across a finite length of the fuselage and are added to the distributed structural weight. The applied loads include the nose landing gear during a hard landing and the force acting on the horizontal tail during a high-g pull up maneuver. All of these forces are continuously summed along every inch of the fuselage to calculate the shear stress at each point. From this it is clear the minimum shear stress will occur at the nose and tail of the airframe, while the maximum is seen at the fuselage station corresponding to the wing spar. The moment acting on the airframe is calculated in a similar fashion. The shear stress is summed up along every inch of the fuselage resulting in a maximum moment applied at the wing spar.

Structural Analysis – Compression and Tensile Stress Limit

The compression and tensile stress limits are the prescribed maximum axial load capacities of an individual member as set forth by the MIL-HDBK-5J.[19] These values are known as the ultimate material tensile stress (F_{tu}), material tensile yield strength (F_{ty}), and material compressive yield stress (F_{cy}).[19] These limits come into play when a load is applied to the fuselage. For example, when a moment is applied to the airframe, one side of the structure is in compression, while the other side is in tension (see Figure 3). It is under these conditions that the applied load cannot result in compression or tensile stresses exceeding that of the MIL-HDBK-5J values,[19] de-rated to meet the CFR guidelines.[20] [21] If these values are exceeded the airframe is at risk of collapse or tension failure.

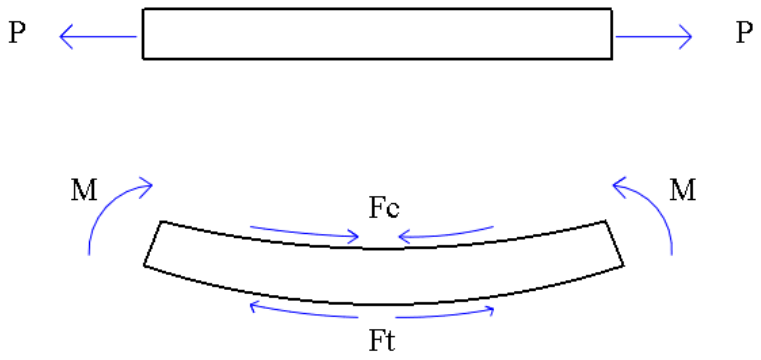

Figure 3. Tensile and Bending Stress Configurations

The compression and tensile stresses within a member are calculated using Equation 1 and the flexure formula (Equation 2), which calculate the stress distribution acting on a given cross section.

$$F_t = \frac{P}{A} \quad (1)$$

$$F_t = \frac{M \cdot c}{I} \quad (2)$$

Where force (P) is in units of lbf, area (A) is in units of in^2, moment (M) is in units of lbf-in, distance from the neutral axis (c) is in units of in, and moment of inertia (I) is in units of in^4. These values combine to solve for the tensile stress (F_t) which is in units of lbf/in^2.

These values are tabulated for each member and cross referenced with the MIL-HDBK-5J [19] to gauge the design feasibility. If the applied loads result in compressive or tensile stresses exceeding the design limits, the design is deemed infeasible, and an alteration must be made.

Structural Analysis – Shear Stress Limit

Shear stress limits are the prescribed maximum load capacity of an individual member in shear. The maximum stress values are again the ultimate material strength and material yield stress limits as set forth by the MIL-HDBK-5J,[19] as well as the buckling and crippling criteria, de-rated according to the CFR.[20] [21] Shear stress is the result of a shear or torsional force acting on a structure. In a semi-monocoque structure the skin carries or transfers the shear loads into the stiffening components and must be sized appropriately. To determine the shear flow in the fuselage skin, the shear force is calculated for each bay. The program then creates a shear build up including shear and compressive forces acting on each stringer. Using Equation 3, the shear flow due to bending is calculated using the geometrical features of the stringers.

$$\bar{q} = \frac{P}{I} \sum y A_s \quad (3)$$

The force (P) is the shear force acting on the stringer, which changes based on location. Again the shear force is in units of lbf, the area of the stringer (A_s) is in units of in^2, and the distance from the neutral axis (y) is in inches. These values combine to solve the shear force which is in units of lbf/in^2 (see Figure 4).

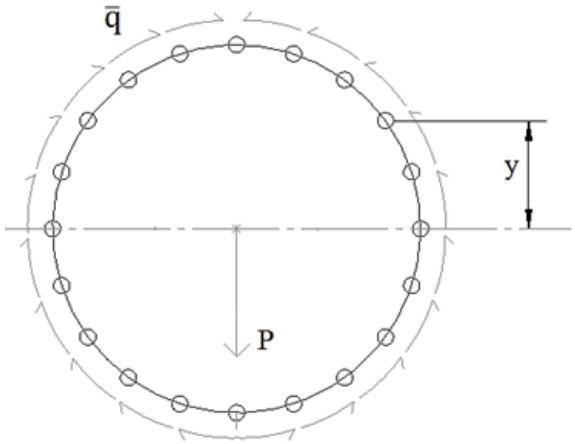

Figure 4. Fuselage Shear Flow

From this, the acting shear stress is simply calculated using the skin thickness as shown in Equation 4.

$$F_{xy} = \frac{\bar{q}}{t} \tag{4}$$

The shear stress values are tabulated for each stringer, along with the shear flow present on each panel, and cross referenced with the MIL-HDBK-5J material limits and the buckling and crippling criteria for curved panels and long column beams.[19] If these values exceed the material stress limits, or the buckling and crippling criteria, the airframe is deemed infeasible and a design alteration is required.

Structural Analysis - Hoop Stresses

Hoop stresses are the result of cabin pressure loads acting on the fuselage skin and frames. This pressure force is a byproduct of the pressure differential between atmospheric pressure and internal cabin pressure and is taken into account when sizing the skin and frames. Using the pressure load, radius of the fuselage, and the thickness of the skins, the hoop stress is calculated using Equation 5.

$$F_{hoop} = \frac{\Delta P r}{t} \tag{5}$$

Where the pressure differential (ΔP) is in units of lbf/in^2, and the radius and thickness are in inches (see Figure 5).

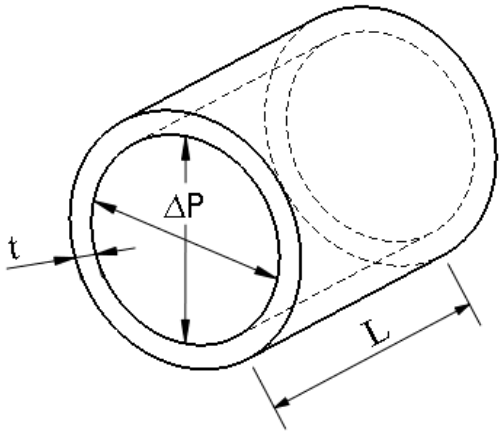

Figure 5. Pressure Vessel Schematic

Structural Analysis - Compression Buckling of Curvilinear Stiffened Panels

Niu [18] references typical buckling constants used throughout the industry. He provides charts useful in determining the compression and shear buckling constants for curved plates and circular cylinders. These charts are digitized into Microsoft EXCEL to

enable their use within the program. From there, a polynomial curve fit is applied to numerically reproduce the chart (see Figure 6 and Figure 7).

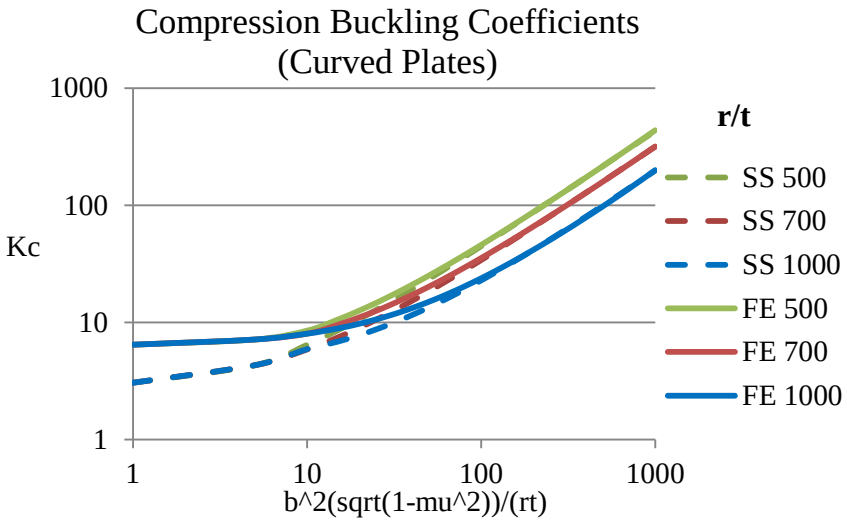

Figure 6. Compression Buckling Coefficient Plot

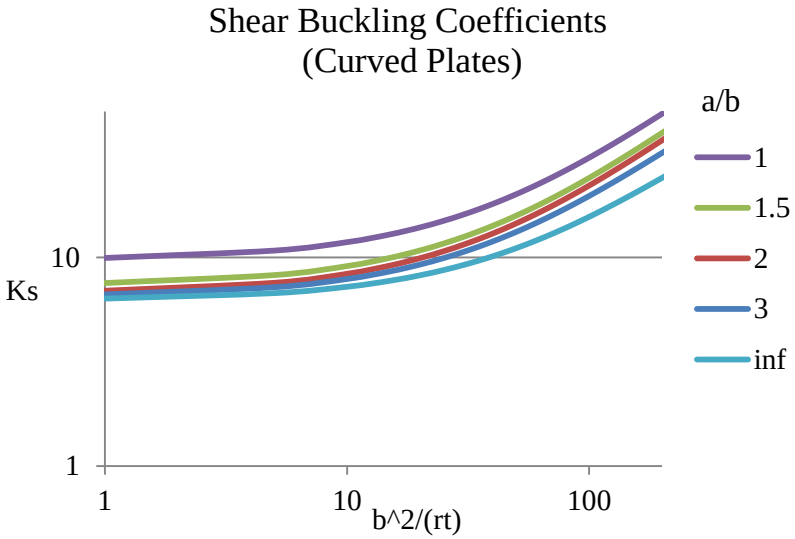

Figure 7. Shear Buckling Coefficient Plot

This creates a grid of data from which a bi-linear interpolator is used to pinpoint the correct buckling constants. Using these buckling constants, Equation 6 and 7 are used to determine the load required to buckle the skin between the frame and stringers

$$F_c = K_c \left(\frac{\pi^2 E}{12[1-\mu^2)}\right)\left[\frac{t}{L}\right]^2 \quad (6)$$

$$F_{cr} = K_s E(t/b)^2 \quad (7)$$

Where the Young's Modulus (E) is in lbf/in^2, and thickness (t), length (L) and frame spacing (b) is in inches. Any load that exceeds this maximum strength threshold results in the skin buckling. Therefore, the program determines whether or not the design input is adequate for the desired loads. If it is not, a thicker skin or closer frame and stringer spacing is required.

A similar technique is used to solve for the buckling and crippling stress within the stringers. This component is arguably one of the most important as it, along with the skin, carries the majority of the primary load.[18] Therefore, it is critical to ensure this component does not fail due to local crippling or buckling stress. In the interest of simplifying the design tool, a *Z*-stringer geometry (see Figure 8) is chosen for the analysis.

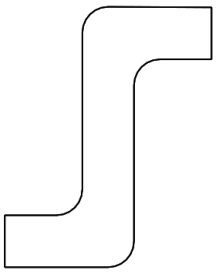

Figure 8. *Z*- Stringer Geometry

The first step in the stringer analysis is to calculate the crippling stress as it is used in buckling equations later on. The technique used to analyze the stringer crippling stress was developed by R.A. Needham [24] and involves summing up the crippling stress of individual angled sections. This requires the stringer geometry to be cut into 90-degree sections, which in the case of the *Z*-stringer, results in two angled sections with the horizontal cut occurring at the middle of the stringer web. Similar to the skin buckling equations, Needham's crippling equations (see Equation 8) require the use of a constant coefficient. This time the constant is dependent on the end fixity (*Ke*=0.366 for fixed edges and *Ke*=0.342 for one edge free). In the case of the *Z*-stringer, only one side is considered "free", so the *Ke*=0.342 constant is fixed. Using the basic stringer geometry and Equation 8 the crippling stress capacity of the stringer is calculated.

$$F_{cs} = \frac{K_e\sqrt{EF_{cy}}}{(b'/t)^{0.75}} \tag{8}$$

$$\text{Where, } \frac{b'}{t} = \frac{a+b}{2t}$$

Where Young's Modulus (E) is in units of lbf/in^2, and a, b, and thickness (t) are in units of inches. Again, this equation determines the absolute maximum stress capacity of the fuselage stringers. Similar to the ultimate structural loads, the crippling stress value is also subject to a 1.5 factor of safety. Therefore, the design crippling load is less than the absolute maximum crippling load. If the applied load exceeds the design capability of the stringer, the user must either increase the material thickness or alter the overall dimensions.

The stringer buckling stress is calculated in a similar fashion using the Euler column buckling equations. The constants are again based on the end fixity (c=1 for simply supported and c=4 for clamped) (see Figure 9).

Column Shape and End Condition		End Fixity Coefficient	Column Shape and End Condition		End Fixity Coefficient
	Uniform column, axially loaded, pinned ends	$c = 1$ $\frac{1}{\sqrt{c}} = 1$		Uniform column, distributed axial load, one end fixed, one end free	$c = 0.794$ $\frac{1}{\sqrt{c}} = 1.12$
	Uniform column, axially loaded, fixed ends	$c = 4$ $\frac{1}{\sqrt{c}} = 0.50$		Uniform column, distribution axial load, pinned ends	$c = 1.87$ $\frac{1}{\sqrt{c}} = 0.732$
	Uniform column, axially loaded, one end fixed, one end pinned	$c = 2.05$ $\frac{1}{\sqrt{c}} = 0.70$		Uniform column, distributed axial load, fixed ends	$c = 7.5$ $\frac{1}{\sqrt{c}} = 0.365$
	Uniform column, axially loaded, one end fixed, one end free	$c = 0.25$ $\frac{1}{\sqrt{c}} = 2$		Uniform column, distributed axial load, one end fixed, one end pinned	$c = 6.08$ (approx.) $\frac{1}{\sqrt{c}} = 0.406$

Figure 9. End Fixtivity Constants. Reproduced from Niu, M., *Airframe Structural Design*, 2nd ed., Hong Kong Conmilit Press LTD, Hong Kong, 2011, pp. 122

These constants assume an axially loaded uniform column, which is a reasonable assumption for aircraft stringers.[17] Depending on the frame spacing and overall stringer dimensions, the long or short column buckling equations are utilized. This decision is based off of the ratio of effective column length to the column radius of gyration (ρ). The critical value is calculated using Equation 9.

$$(L'/\rho)_{critical} = \sqrt{2}\pi\sqrt{E/F_{cs}} \quad (9)$$

Where, $\rho = \sqrt{\frac{I}{A}}$

If the ratio of stringer length to radius of gyration is less than the critical value, the short column equation is used, and visa-versa. The long column equation (Equation 10) is solely based off of the chosen material and stringer geometry. The short column equation (Equation 11), on the other hand, utilizes the previously calculated crippling stress as well as the material properties and stringer geometry.

$$F_c = \frac{c\pi^2 E}{(L/\rho)^2} \quad (10)$$

$$F_c = F_{cs}\left[1 - \frac{F_{cs}(L\prime\rho)^2}{4\pi^2 E}\right] \quad (11)$$

Again, similar to the crippling stress, the ultimate buckling strength is also subject to a 1.5 factor of safety. However, due to the fact the crippling stress is already de-rated, this additional 1.5 is only applied to the buckling stress if the long column equation (Equation 10) is used. Recall the long column equation has no dependence on the crippling stress; therefore, the 1.5 factor of safety must be applied to calculate the design buckling strength. By comparing the design buckling and crippling stress values, it is easy to determine whether or not the structure is buckling or crippling dominated and adjustments can be made accordingly. If the structure is found to be inadequate the program iterates between different geometry sizes until an adequate structure is found.

The last piece of the semi-monocoque structure is the frames. This piece of structure is critical in maintaining the shape of the pressurized fuselage as well as limiting the length of the stringer sections. The spacing between frames plays a large role in overall skin thickness and stringer sizing. Obviously, the smaller the frame spacing, the

larger the compressive load capacity of the skins and stringers. Unfortunately, these benefits carry a weight penalty as more frames are required with decreased frame spacing. Therefore, a balance must be found between frame spacing and overall structural geometry. Again, in the interest of simplifying the design tool, a basic *I*-frame, with equal upper and lower cap width, is the only geometry considered (see Figure 10).

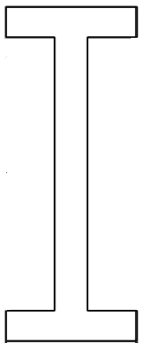

Figure 10. *I*- Frame Geometry

Utilizing Equation 12, a preliminary minimum sizing requirement for the frames is calculated. This equation is found in Niu's [18] structural design handbook and takes into account the frame spacing, applied moment, and fuselage geometry to determine the frame sizing.

$$\mathrm{EI} = \frac{\mathrm{MD}^2}{16000\mathrm{L}} \tag{12}$$

Where the fuselage diameter (D) and length (L) are in inches. Solving this equation for the area moment of inertia (I), the overall cross-section dimensions of the frame are calculated. This is done within the program by iterating between pre-defined frame geometries until an adequate geometry is found.

SUMMARY OF DESIGN LOADS

The aircraft fuselage design largely depends on the loads applied to the structure. These loads are determined based on the desired performance capability of the finished product. From these requirements the aerodynamic, inertial flight, pressure, and landing loads are derived.

Point Mass Loads

Every aircraft has a multitude of point mass loads which must be accounted for in the structural sizing. These loads consist of items such as passenger furnishing, engines, payload, tail structure, etc. Each load is evenly spread across the fuselage based off of their size. The engines, for example, could be 4-ft long and weigh 1,000-lbm, resulting in 20.8-lbm/in spread across the location corresponding to the engines. While the weight of some components must be estimated by the user, some are estimated empirically from a set of weight equations found in Niu's design textbook.[25]

The empirical weight for the empennage structure is estimated based off the tail geometry and limit speeds using Equation 13 and 14 below,

$$W_{HT} \approx k_{HT} \cdot S_{HT} \left(3.5 + 2 \frac{S_{HT}^{0.2} \frac{V_D}{\sqrt{\cos(\Lambda_{HT})}}}{1000} \right) \tag{13}$$

Where, k_{HT} is 1.0 for fixed horizontal tails, 1.1 for inverted T-tails, and 1.19 for variable incidence T-tail configurations.

$$W_{VT} \approx k_{VT} \cdot S_{VT} \left(3.5 + 2 \frac{S_{VT}^{0.2} \frac{V_D}{\sqrt{\cos(\Lambda_{VT})}}}{1000} \right) \tag{14}$$

Where, k_{VT} is 1.0 for inverted T-tails, and 1.15 for T-tail configurations. For both Equation 13 and 14, the tail surface areas (S_{HT} and S_{VT}) are in units of ft^2, the dive speed (V_D) is in knots indicated airspeed (KIAS), and the sweep angle (Λ) is in radians. These values combine to solve for the weight of the vertical and horizontal tail which is units of lbm. From each of these equations, it is clear the weight of the empennage will increase as the surface area of each tail increases.

The empirical weight of the nose gear is estimated based off of the aircraft MTOW and wing configuration using Equation 15 below,

$$W_{NG} \approx k(20 + 0.1 \cdot MTOW^{0.75} + 0.000002 \cdot MTOW^{1.5}) \quad (15)$$

Where, k is 1.0 for low-wing aircraft and 1.08 for high-wing aircraft. Both weights (MTOW and W_{NG}) are in units of lbm. This equation ensures the landing gear weight increases with the size of the aircraft as would be expected.

The empirical weight of the cockpit instruments is estimated based off of the aircraft's design range and OEW using Equation 16 below,

$$W_{Inst} \approx 0.575 \cdot OEW^{0.55} \cdot DR^{0.25} \quad (16)$$

Where, OEW is in units of lbm, and the design range (DR) is in units of nautical miles. The weight of the instrumentation (W_{Inst}) is in units of lbm. It makes sense that a larger aircraft, with a more expansive cockpit, would have more instrumentation. Thus, the instrument weight increases as the OEW and design range increase.

The empirical weight of the passenger furnishing is estimated based off of the desired furnishing and capacity of the aircraft using Equation 17.

$$W_{PF} \approx C \cdot NPass \quad (17)$$

In this equation, C is 40-lbm for basic commercial interior, and 75-lbm for first class or business interior. As the number of passengers increases, the number of seats also increases, thus increasing the passenger furnishing weight.

Finally, the passenger payload is estimated based on the number of passengers, flight length, and additional crud weight using Equation 18.

$$\text{Payload} \approx \text{W} \cdot \text{NPass} + \text{EW} \tag{18}$$

In this equation, W is 190-lbm for commuter flights, 215-lbm for domestic flights, and 280-lbm for international flights. This weight includes the basic passenger weight, as well as luggage weight based on the flight distance. The additional crud weight (EW) accounts for food, potable water, and other items essential to a commercial flight. This value is assumed to be 150-lbm for commuter and domestic flights, and 215-lbm for international flights.

Cabin Pressure Loads

As with any pressurized cabin there exists a pressure differential between the outside ambient air and the inner cabin pressure. This differential creates a pressure load which must be accounted for in the frame and skin sizing. To calculate this load, a differential pressure is calculated between the ambient pressure, at the desired cruising altitude, and the internal cabin pressure. These pressures are found using a standard atmosphere table and assuming ambient conditions.

According to 14 CFR § 25.365 [26],

> "The airplane structure must be designed to be able to withstand the pressure differential loads… multiplied by a

factor of safety of 1.33 for airplanes to be approved for operation to 45,000 feet or by a factor of 1.67 for airplanes to be approved for operation above 45,000 feet."

This regulation adds an additional factor of safety to the already applied 1.5 factor of safety required by 14 CFR § 25.303 [20]. The pressure loads for 6,000-ft and 8,000-ft cabin altitudes can be seen in Figure 11. It is important to notice the distinct jump in design pressure loads at 45,000ft as the factor of safety increases from 1.33 to 1.67.

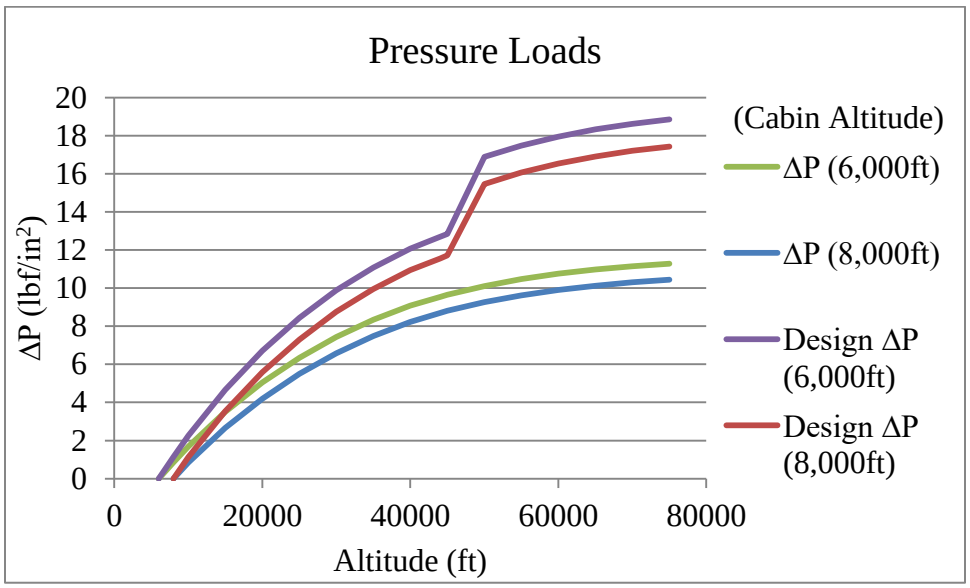

Figure 11. Cabin Pressure Loads

After applying the appropriate factors of safety the overall pressure load is used to determine the hoop stress acting on the frame and skin structure (recall Equation 5).

Flight Loads

Flight loads play a large role in the adequate sizing of the airframe structure. These flight loads are considered the maximum steady maneuvering loads governed by the V-N diagram (14 CFR § 25.337[27]). The V-N diagram specifies limit loading environments experienced by the airframe; they correspond to flight at stall, cruise, and maximum dive speed. These loads are taken into account within the program by multiplying the inertial loads by the user prescribed flight loading.

Positive Flight Loading

The positive flight load acting on an aircraft is defined according to 14 CFR § 25.337 (b) [27] which states,

> "The positive limit maneuvering load factor *n* for any speedup to Vn may not be less than 2.1+24,000/ (W+10,000) except that n may not be less than 2.5 and need not be greater than 3.8…"

For most aircraft certified under part 25, this results in a positive maximum limit maneuvering load of +2.5g; however, a larger maximum load can be specified by the designer for use in this tool. Typical commercial aircraft stick to the bare minimum to minimize structural weight and improve fuel efficiency. Military or acrobatic aircraft, on the other hand, typically require much larger maximum load capacity upwards of +6g. Therefore, the ability to specify specific maximum load capacity has been left up to the user's discretion. A representation of how the positive flight loading changes with weight can be seen in Figure 12.

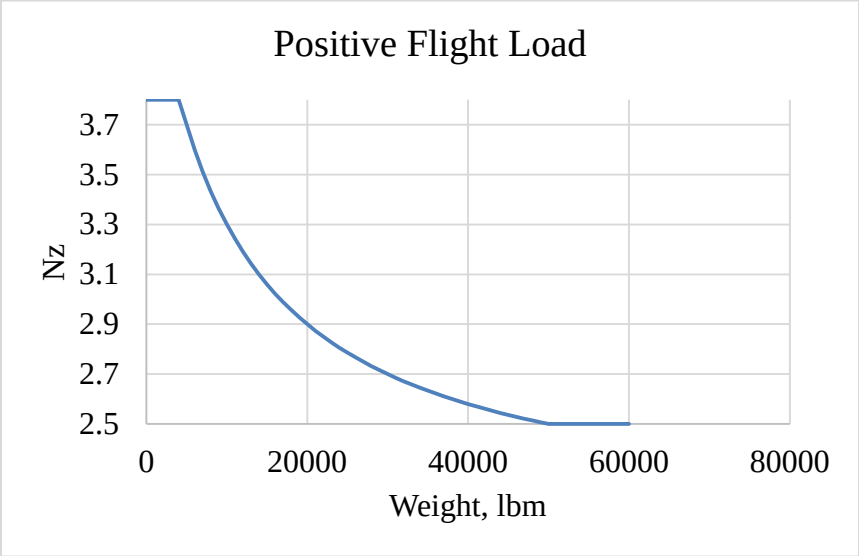

Figure 12. 14 CFR § 25.337 [27] Positive Flight Loading

Negative Flight Loading

The negative flight load capacity is governed by 14 CFR § 25. 337 (c) [27] which states,

> "The negative limit maneuvering load factor may not be less than -1.0 at speeds up to V_C…Must vary linearly with speed from the value at V_C to zero at V_D…Factors lower than those specified in this section may be used if the airplane has design features that make it impossible to exceed these values in flight "

This usually results in a minimum -1-g loading applied to the airframe. Due to the nature of the human body, most civilian designs stick to -1-g loading, as anything over this is detrimental to the passengers and pilot.

Tail Loads

An aircraft's empennage imparts large vertical and horizontal forces at the rear of the fuselage. This in turn, creates a large moment about the wing spar due to the tail's long moment arm. The load used in this analysis equates to the necessary trim loads for steady flight. The maximum trim load is found in the event of a rapid decompression event when the aircraft is forced to quickly dive below 10,000-ft. This load is calculated based on the aircraft's coefficient of lift (CL), maximum flight load (Nz), wing surface area (Sref), mean geometric chord, tail moment arm, dynamic pressure (at 10,000ft and the aircraft's maximum dive speed) and assumed aircraft stability. For the purpose of this analysis, the aircraft is assumed to have a CG location rendering the airframe 35% stable. Using these values the tail load to trim an Nz pull up at maximum dynamic pressure, is calculated using Equation 19, 20, and 21.

$$\mathrm{CL} = \frac{\mathrm{Nz} * \mathrm{W}}{\mathrm{Sref} * \mathrm{q}} \tag{19}$$

$$\mathrm{Cm} = 0.35 * \mathrm{CL} \tag{20}$$

$$\mathrm{TL} = \frac{\mathrm{Cm} * \mathrm{q} * \mathrm{Sref} * \bar{\mathrm{c}}}{\mathrm{l}} \tag{21}$$

In these equations the weight (W) is in lbm, the Sref is in ft^2, the mean geometric chord ($\bar{c}$) and tail moment arm (l) are in feet, and the dynamic pressure is in units of lbf/ft^2. The dynamic pressure, in this case, is solved from the maximum dive speed which is in knots indicated air speed (KIAS). Equation 22 is used to convert this value into lbf/ft^2 for use in Equation 19 and 21.

$$q = 1481 \left(\frac{V_D}{660.8}\right)^2 \tag{22}$$

The 660.8 value converts the maximum dive speed from feet per second into knots indicated airspeed (KIAS), while 1,481 represents the dynamic pressure per Mach squared (q/M^2) at sea level. Combined, these values solve for the dynamic pressure in units of lbf/ft^2.

Landing Loads

Loads imparted by the landing gear also play a key role in the structural design. The impact of both the main and nose gear on a hard landing impact the sizing of structure throughout the aircraft, especially the wing spar and local frames and stringers. To simulate a hard landing scenario, the nose gear is assumed to smack into the runway harder than it normally would on a smooth landing, imparting a large applied load at the front of the aircraft. Again, this load is estimated by the user and taken into account based on their input. In this program, due to the assumption of "grabbing" the fuselage at the wing spar, the loads applied by the main landing gear are not taken into account, as they are typically tied into the wing spar structure.

IMPLEMENTATION OF DESIGN PROCESS

One of the many challenges of putting together a design tool concerns the "curse of dimensionality": because "everything affects everything." A small change in one area ripples throughout the design and affects everything else. This can result in either a positive or negative structural impact. In an abstract sense, the optimal structural layout can only be found where all design variables are truly independent. An explosively large number of candidate designs must be evaluated if all possible combinations are enumerated. A rule based design process can radically reduce the number of independent design variables, because many dimensions and thicknesses become well defined functions of a few truly independent variables.

The first component sized by the program is the fuselage skin. The program determines the required skin thickness based off of the pressurization loads taking into account the CFR factors of safety. This sizing is considered the minimum required skin size. Later, within the panel shear build up calculations, the skin is again analyzed to ensure the shear stress in each panel does not exceed the buckling and crippling criteria. If this value is exceeded, the skin is resized until the stress is lowered into these bounds. The program includes a number of different skin thickness cases ranging from 0.032in (20 gauge) up to the extreme of half an inch. If the program is unable to find an adequate sizing from these options, the user prescribed inputs are deemed infeasible.

Next, the frames are sized utilizing the moment applied at each frame station. As previously discussed, the fuselage structure is split into forward and aft sections based off the location of the wing spar. The fuselage is again split into frame stations based off of the frame spacing and overall fuselage length. Next, the maximum force at each frame

station is calculated and used to determine the minimum area moment of inertia required for each frame. Starting with the minimum geometry size, the program iterates through a number of sizing cases until the required frame geometry, with the appropriate area moment of inertia, is found. Unlike the skin and stringers, the frame sizing is largely decoupled from the rest of the structure.

Finally, the program calculates the stringer sizing based off of the compression and shear forces acting at each stringer location. To begin, the program assumes each stringer to have the minimum allowable sizing. This helps ensure the airframe is not oversized and minimizes the overall weight. Due to the nature of the shear and compression force build up, each stringer affects the sizing of subsequent members. For example, in the upper and lower stringers, which see the largest compression force due to bending, the minimal stringer size results in a large compression force at these locations. If the stress is over the buckling, crippling, or material strength limits the program increases the size of the stringer until the stress drops below these requirements. This in turn affects the stress seen in the subsequent stringer, as it is still set at the smallest stringer geometry, and is now picking up a different stress loading. This stress redistribution continues as the program systematically moves around the fuselage and resizes the stringers until each member is under the stress requirements.

After each component is optimally sized, the program outputs the geometry sizing for each member which is easily transferred into the parameterized CAD template. To simplify the CAD model, the skin is considered constant for the entire length of the fuselage. This assumption is considered adequate as the structure analyzed in this program does not have any cutouts or voids and the pressurization load is constant

throughout. The CAD template utilizes the overall length, diameter, and skin thickness parameters, and automatically resizes the structure to meet the new dimensions.

The stringers are also considered to be constant geometry based off of the worst case scenario for each stringer location. This worst case is seen near the wing spar where the stress is highest. Therefore, the geometry at this location is carried through the entire length of the stringer. The CAD template is split into the number of different stringers, each parameterized to accept web height, cap width, and material thickness. If these parameters are altered, the program automatically resizes to meet the new dimensions.

Finally, the frame geometry is designed to change at each frame station. The CAD template adds or deletes frames based off of the overall fuselage length and frame spacing parameters. Each individual frame is parameterized to accept the web height, cap width, and material thickness.

The next step in the process is to import the CAD structure into FEA analysis software (ANSYS). This program is used to verify and fine tune the results obtained from the structural analysis tool. To minimize the overall size of analysis run in ANSYS, the fuselage section closest to the wing spar is analyzed, subjected to the worst loading case. These results determine whether or not the remaining structure is sized correctly.

RESULTS

The structural design tool is designed to handle a wide range of aircraft sizes varying from small business jets up to wide body commercial jets. To test the functionality of the program, an analysis was conducted at both ends of the spectrum. While many of Niu's [17] [18] structural design methods are based off of larger aircraft, a number of design factors and minimum sizing requirements are added to ensure accurate sizing of smaller platforms. As will be discussed later on, the structure of the smaller business sized aircraft often sat around the minimum sizing thresholds, while the larger wide body aircraft fluctuated based off the strength based requirements of the airframe. After sizing the individual airframes, the structure was modeled in CAD software and verified using FEA.

Business Jet Analysis

To test the program functionality on smaller aircraft platforms, an analysis based on aircraft in the "super mid-sized" business jet category is conducted. These aircraft typically include fuselage sizes in the neighborhood of 60-70-ft long and 80-90-in wide and a Maximum Takeoff Weight (MTOW) of approximately 30,000-lbm.

Design Inputs

The first step in the analysis process is supplying the program with all of the design variables. To ensure accurate structural sizing, it is critical to ensure all inputs are accurate and approximate weights are appropriate to the aircraft size. The input variables range from basic fuselage dimensions, cabin and cruising altitude, estimated point

masses, as well as estimated tail and landing loads. As previously discussed, all of the these estimates are based off of published data for jets in this category, in addition to point mass estimates based off of Niu's [17] [18] design handbook.

Business jets in the "super mid-sized" category are typically in the neighborhood of 60-70-ft long and 80-90-in wide, so a 62-ft long and 90-in wide airframe was chosen for this analysis. Next, based off of Niu's [18] tabulated data on typical aircraft sizing, the stringer and frame spacing is set to ~7-in and 20-in respectively. This spacing results in 40 stringers equally spaced around the fuselage and 37 frame stations. In addition to the point masses (discussed later) an approximate structural weight of 8,000-lbm is spread across the entire fuselage. A complete list of these parameters can be seen in Table 3.

Table 3. Business Jet: Sizing Inputs

Fuselage	
Length	744 in
Diameter	90 in
Frame Spacing	20 in
Number of Stringers	40
Wing Spar Location	375 in
Est. Structural Weight	8,000 lbm

One of the primary forces acting on an aircraft's structure is the internal cabin pressure. This pressure is based off of the aircraft cruising altitude, and desired cabin altitude. Aircraft in this category have service ceilings ranging from around 40,000-ft up to 50,000-ft, and cabin altitudes as low as 5,000-ft. A service ceiling of 45,000-ft is used for this analysis with a cabin altitude of 5,960-ft. Using a standard atmosphere the positive and negative pressurization loads are calculated to be 9.89-lbf/in^2 and 0.5-lbf/in^2 respectively. According to 14 CFR § 25.365 [26], a 1.33 FOS must be applied as the

aircraft is designed to fly at or below 45,000-ft. Applying this FOS to the previously calculated pressurization loads results in a positive pressurization load of 13.16-lbf/in^2 and negative pressurization load of -0.665-lbf/in^2 applied to the structure.

The next primary force comes from the flight loads. These loads are based on 14 CFR § 25.337 (b) and (c) [27] and an estimated MTOW. As previously mentioned, aircraft in this category have MTOW's in the neighborhood of 30,000-lbm. Therefore, an MTOW of 30,000-lbm is used for this analysis. According to 14 CFR § 25.337 (b), [27] this results in a positive flight load of +2.7-g applied to the airframe.

The tail and landing loads are estimated based off of the aircraft dimensions, flight conditions, and basic airfoil geometry. To calculate an approximate tail loading, an estimated dynamic pressure is calculated based off of the maximum dive speed and altitude estimated to be 400-KIAS and 10,000-ft respectively. Using a standard atmosphere table, the dynamic pressure is calculated to be 543-lbf/ft^2. These numbers equate to a rapid decompression event where the aircraft is forced to rapidly dive below 10,000-ft. The aircraft is assumed to have a wing reference area of 537-ft^2, wing mean geometric chord of 7.8-ft, and tail moment arm of 22.9-ft (based on the tail and wing spar locations). Using these parameters the horizontal trim load is calculated to be 9,932-lbf to enable a +2.7-g pull up at maximum dynamic pressure (400 KIAS). A summary of all estimated flight, tail, and landing loads used in this analysis can be seen in Table 4.

Table 4. Business Jet: Applied Loads

Flight	
Flight Load	+2.7 g
Landing	
Nose Gear	4,000 lbf
Tail	
Horizontal	9,932 lbf
Pressure	
Positive	13.162 lbf/in^2
Negative	-0.665 lbf/in^2

The next primary force applied to the airframe comes from the point mass loads. These loads include a combination of published weights, empirically estimated weights,[25] and approximate component weights. Aircraft in this category typically have a seating capacity between 9-12 passengers, so the payload estimates account for 12 international passengers. Approximate weights include two pilots estimated at 175-lbm each, cockpit furnishing estimated at 200-lbm, and a single aft lavatory estimated at 250-lbm. A complete summary of weights along with their respective locations can be seen in Table 5.

Table 5. Business Jet: Point Masses

Component	Location Start (in)	Location End (in)	Weight (lbm)
Avionics	12	36	935
Cockpit Furnishing	48	100	200
Pilots	60	72	350
Passenger Furnishing	100	400	900
Payload	100	500	2,735
Engines	500	548	2,300
APU	700	747	300
Lavatory	400	460	250
Nose Gear	60	65	265
Vertical Tail	600	700	620
Horizontal Tail	600	700	890

To accurately size the structure, each component is assigned a material. In this analysis, Aluminum 2024-T3 is used for aircraft skin due to its high fatigue strength, while Aluminum 7075-T6 is used for the frames and stringers due to its high tensile yield strength. A summary of material choices can be seen in Table 6 .

Table 6. Business Jet: Material Choices

Material	
Skin	Aluminum 2024-T3
Stringer	Aluminum 7075-T6
Frame	Aluminum 7075-T6

Program Outputs

Now that the initial setup is complete, the program utilizes the user supplied inputs to design and size a conceptual aircraft fuselage. The first step is calculating the required skin thickness. To ensure the aircraft skin is thick enough for the desired cabin altitude, the program calculates the hoop stress and compares it with the material characteristics. If the stress is above the yield strength, taking into account appropriate factors of safety, the skin thickness is increased and the process repeats. In this analysis, Aluminum 2024-T3 is used for the skin material resulting in a maximum yield strength of 42,000-lbf/in^2, which is de-rated to 28,000-lbf/in^2 after applying the 1.5 FOS according to 14 CFR § 25.303.[22] The full sizing process can be seen in following example:

$$F_{Hoop} = \frac{(13.16\ lbf/in^2\ )(45in)}{0.032in} = 18{,}506\ lbf/in^2$$

$$F_{Design} = \frac{42{,}000\ lbf/in^2}{1.5} = 28{,}000\ lbf/in^2$$

$$F_{Hoop} < F_{Design} \rightarrow T_{skin} = 0.032in$$

From this analysis it is clear the minimum gauge skin thickness results in a hoop stress far below the material design limits. Therefore, the skin thickness is set to a minimum gauge thickness of 0.032-in (20-gauge).

Next, the program calculates the maximum panel buckling strength using the previously calculated skin thickness. Each panel is comprised of five components: two stringers, two frames, and the skin in between. Utilizing the frame and stringer spacing of 20-in and ~7-in respectively, the program interpolates and records both shear and compression buckling coefficients. These coefficients, along with the material

characteristics, are used to calculate the maximum allowable stress on the skin (see Table 7**).**

Table 7. Business Jet: Initial Panel Buckling Strength

Type	Coefficient	Strength (lbf/in^2)
Compression	3.60	774.69
Shear	11.39	2450.42

As will be shown later in this section, these strength values are used to verify the skin thickness by applying maximum strength boundaries. If an applied force is found to exceed these values, a design alteration must occur.

Next, the program sizes the frames. Each frame is sized according to the forces acting at each individual frame station. Using the overall fuselage length and the frame spacing, the fuselage is divided into 37 frame stations with 18 in the forward section of the aircraft and 15 in the aft. In order to calculate the shear and moment acting on the fuselage, the program first builds a lumped mass model. This model is based on the applied point loads evenly distributed throughout the fuselage based on their location. These raw weights are multiplied by the positive flight load, previously calculated to be 2.7, to create the lumped mass model. The lumped mass models for the forward and aft sections of the fuselage can be seen in Figure 13 and Figure 14.

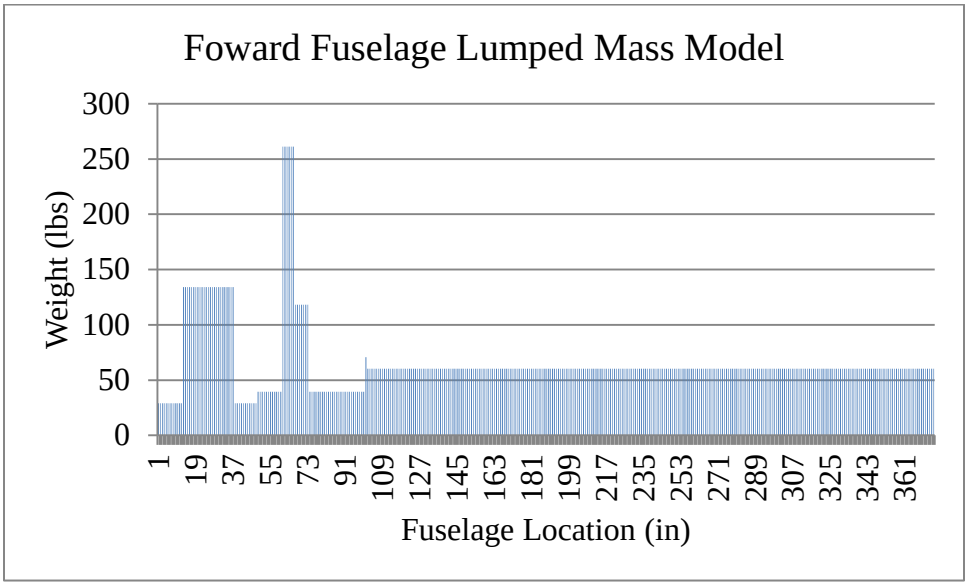

Figure 13. Business Jet: Forward Fuselage Lumped Mass Model

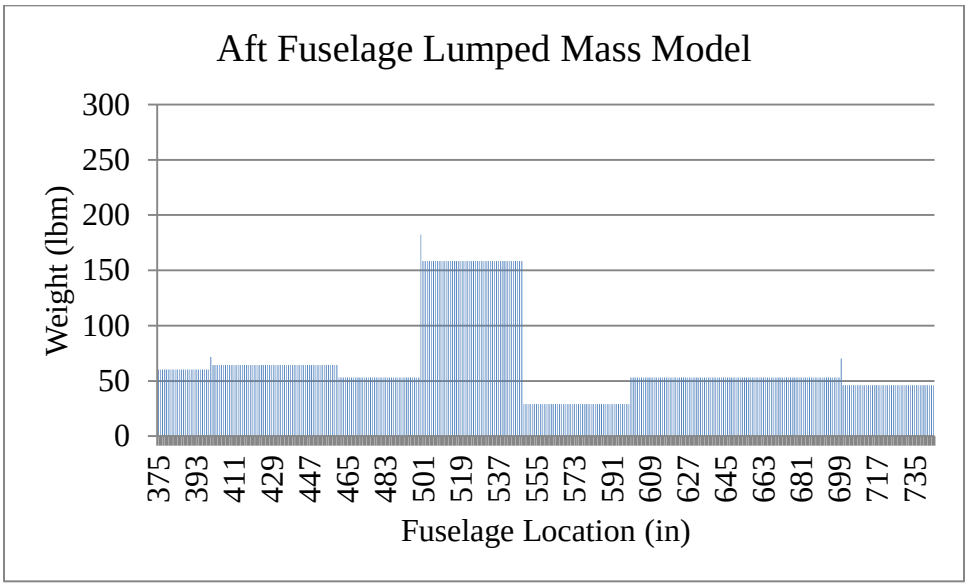

Figure 14. Business Jet: Aft Fuselage Lumped Mass Model

Utilizing the lumped mass model, the program calculates a shear buildup for the forward and aft sections of the aircraft. Each buildup is created by integrating the applied force starting at the nose or tail and ending at the wing spar. The shear force in the

forward section peaks at 29,366-lbf while the aft section peaks at 34,229-lbf. The shear build ups for both fuselage sections can be seen in Figure 15.

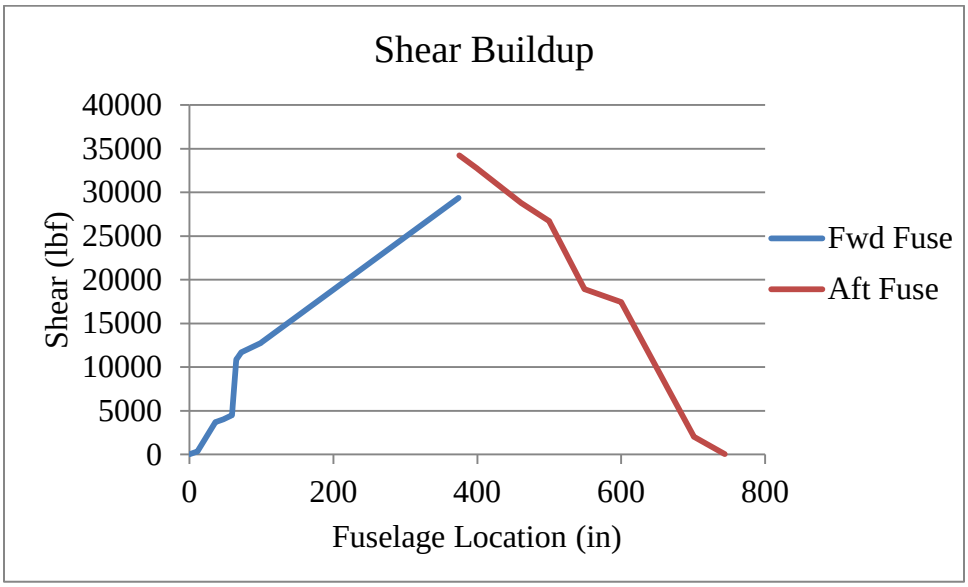

Figure 15. Business Jet: Shear Buildup

A similar process is followed to construct a moment buildup. In this case the shear force is integrated starting at the nose or tail and ending at the wing spar. Similar to the shear buildup, the aft section experiences a slightly higher applied moment compared to the front. The maximum moment in the forward section is calculated to be 6,409,133-lbf·in and 6,885,956-lbf·in in the aft section. The moment build up for each section is shown in Figure 16.

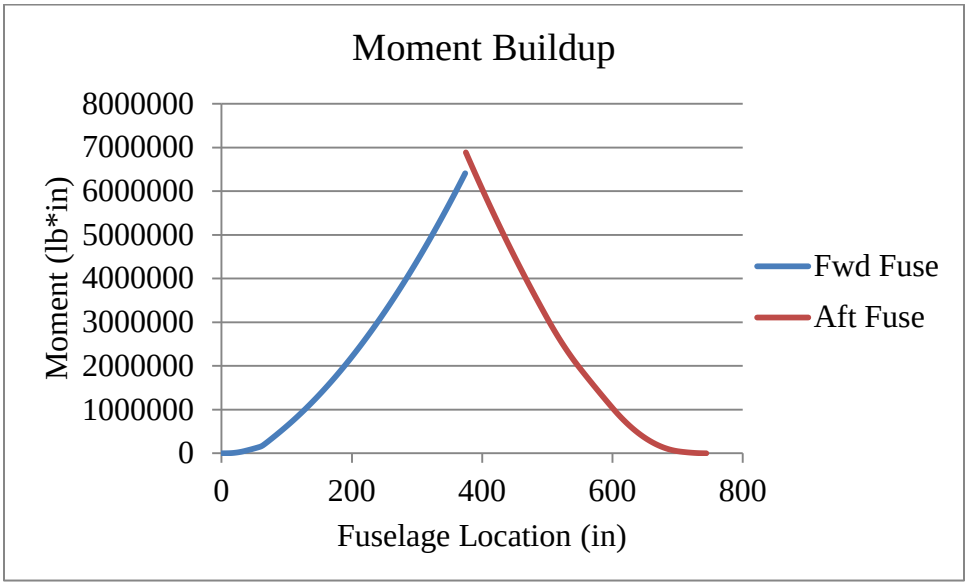

Figure 16. Business Jet: Moment Buildup

A significant assumption in this analysis is the notion of "fixing" the fuselage at the wing spar (recall Figure 2). Unfortunately, the inertial flight loads applied to the airframe are difficult to test on the ground or in this case a computer simulation. In order to calculate the moment and shear forces acting on the fuselage the structure must be fixed at some point. In flight, the aircraft is primarily supported by the wing. To try and simulate an aircraft in flight, the decision was made to fix the structure by the wing spar and pivot all forces around this point. Unfortunately, this assumption leads to force discontinuities between the forward and aft portions of the fuselage. The forward section of the fuselage accounts for the nose gear and applied point masses while the aft portion supports the applied tail loads and the remaining point masses. As was previously discussed, the tail loads far outweigh the nose landing gear loads resulting in a force discontinuity at the wing spar. This discontinuity is not something seen in actual aircraft

as the load path is not interrupted at the wing spar; however, this analysis cannot be conducted without fixing the aircraft at some point.

To size the aircraft frames, the program utilizes the data from the shear and moment buildups to calculate the necessary area moment of inertia for each frame station. Using the required area moment of inertia the program searches the predefined frame options until an optimal size is found. In this case, the required frame size is relatively small due to the aircraft's size and applied loads, and because of this, all frame stations are sized to the minimum frame size. As discussed earlier, minimum sizing requirements are set to ensure smaller aircraft are sized appropriately keeping future manufacturability and system integration in mind. Again, as this is only a conceptual design tool, the program does not take into account larger frames at the wing junction, or web height variations based on system layouts. These adjustments can be made later on in the preliminary design phase. A table displaying the frame dimensions for all 37 frame stations can be seen in Table 8.

Table 8. Business Jet: Frame Dimensions

Station	Cap Width (in)	Web Height (in)	Thickness (in)
1-37	0.75	2.00	0.0641

The final, and most computationally expensive analysis, is the stringer sizing. Taking into account the shear and moment buildups, and aircraft geometry, the program builds an extensive shear buildup to size the stringers. Starting with the minimum stringer sizing, the program calculates the shear and compressive loads on each stringer and compares them to the buckling, crippling, and material limit loads. Using the Needham

crippling and Euler buckling equations, the crippling and buckling stress limits are calculated for all 40 stringers at each of the 37 frame stations. If a stringer size is found to be inadequate, the program increases its dimensions, moves to the remaining stringers, and then starts over. As would be expected, the worst shear loads appear at the longitudinal stations located near the wing spar, thus resulting in the largest stringer sizes at this location. A sample shear buildup at the wing spar location can be seen in Table 9.

Table 9. Business Jet: Sample Shear Buildup (Near the Wing Spar)

Stringer #	Af (in^2)	y (in)	yAf (in^3)	(Y^2)Af (in^4)	Σ(yAf) (in^3)	$\bar{q}_{bending}$ (lbf/in)	Fxy (lbf/in^2)	Fxx (lbf/in^2)
1	0.19	45.00	8.44	379.69				
					8.44	10.10	250.6	10661.3
2	0.38	44.45	16.67	740.79				
					25.10	30.05	745.6	10530.1
3	0.38	42.80	16.05	686.86				
					41.15	49.26	1222.3	10139.5
4	0.38	40.10	15.04	602.86				
					56.19	67.26	1668.9	9499.3
5	0.38	36.41	13.65	497.02				
					69.84	83.60	2074.4	8625.2
6	0.38	31.82	11.93	379.69				
					81.77	97.88	2428.8	7538.7
7	0.25	26.45	6.61	174.91				
					88.39	105.79	2625.2	6266.6
8	0.13	20.43	2.55	52.17				
					90.94	108.85	2701.0	4840.1
9	0.13	13.91	1.74	24.17				
					92.68	110.93	2752.6	3294.5
10	0.10	7.04	0.70	4.96				
					93.38	111.77	2773.6	1667.8
11	0.05	0.00	0.00	0.00				
					93.38	111.77	2773.6	0.0
			SUM	7086.22		MAX	2773.6	10661.3

Due to symmetry, only 11 of the 40 stringers are analyzed with the results mirrored across the *x* and *z* axis. Each stringer is sized based on either the design material strength or the crippling and buckling strength. From Table 9, it is clear the stringers in this analysis are not sized based on material strength requirements. The stringers are made from Aluminum 7075-T6 with a design material yield strength of 46,000-lbf/in^2, well above the maximum compressive force found in this case. Therefore, the stringers are sized based on either the buckling or crippling strength (see Table 10).

Table 10. Business Jet: Stringer Strength Values (Near the Wing Spar)

Stringer #	Crippling Strength (lbf/in^2)	Buckling Strength (lbf/in^2)
1|21	193,141	16,038
2|20|22|40	193,141	16,038
3|19|23|39	193,141	16,038
4|18|24|38	193,141	16,038
5|17|25|37	193,141	16,038
6|16|26|36	193,141	16,038
7|15|27|35	324,824	7,128
8|14|28|34	142,497	7,128
9|13|29|33	142,497	7,128
10|12|30|32	142,497	7,128
11|31	142,497	7,128

From this analysis it is clear the stringers are buckling dominated as the crippling strength is far greater than the design buckling strength. As the analysis progresses through each frame station, the sizing for each individual stringer is stored. When the final frame station has been analyzed, the program outputs the stringer sizing for each individual stringer. A table displaying all stringer dimensions (located near the wing spar) can be seen in Table 11.

Table 11. Business Jet: Stringer Dimensions (Near the Wing spar)

Stringer #	Cap Width (in)	Web Height (in)	Thickness (in)
1|21	0.375	0.75	0.25
2|20|22|40	0.375	0.75	0.25
3|19|23|39	0.375	0.75	0.25
4|18|24|38	0.375	0.75	0.25
5|17|25|37	0.375	0.75	0.25
6|16|26|36	0.375	0.75	0.25
7|15|27|35	0.25	0.50	0.25
8|14|28|34	0.25	0.50	0.125
9|13|29|33	0.25	0.50	0.125
10|12|30|32	0.25	0.50	0.125
11|31	0.25	0.50	0.125

Secondary to the stringer sizing, the program also revisits the skin thickness as it progresses through the stringer shear build up to ensure it can withstand the applied shear forces. This involves comparing the calculated shear forces to stiffened panel buckling criteria (recall Table 7) and adjusting the sizing as necessary. In this case the program found the skin thickness (previously set to 0.032-in based on pressure loads) to be inadequate at this location and resized the skin to 0.0403-in (18 gauge) thick. This results in the new panel buckling limits seen in Table 12.

Table 12. Business Jet: Final Panel Buckling Strength (Near the Wing Spar)

Type	Coefficient	Strength (lbf/in^2)
Compression	3.60	775
Shear	10.40	3,550

Quickly revisiting Table 9, the largest shear stress at the wing spar is 2,773-lbf/in^2, which is less than the maximum panel buckling strength of 3,550-lbf/in^2, verifying the skin is appropriately sized.

It is important to keep in mind this skin and stringer sizing is based on the highest shear stress occurring near the wing spar. The majority of the fuselage skin can be sized purely off of pressurization loads as the shear stress does not exceed the shear buckling limit in most locations. Skin doublers can be implemented in these high stress areas to effectively thicken the skin to 0.0403-in (18 gauge), leaving the rest of the fuselage skin at the previously found 0.032-in (20 gauge) thickness.

At the conclusion of the structural analysis process the program outputs the sizing for each component. These dimensions are transferred to the parameterized CAD model and used to model the full fuselage structure.

CAD Geometry

The CAD model is split into four parametrized components: the skin, frames, stringers, and full assembly. Each component is parametrized to accept the outputs from the structural analysis output. The model is designed to automatically resize according to dimension variations. An example of a parameterized *Z*-stringer can be seen in Figure 17.

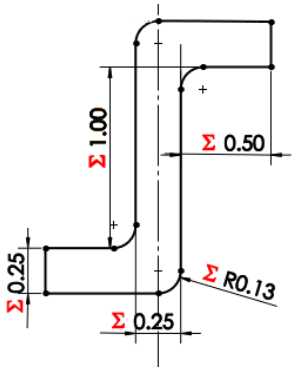

Figure 17. Parameterized *Z*-Stringer

Notice this component is set up to accept web height, cap width, and material thickness. The frames and skin are set up in a similar fashion based on their specific dimensions.

This analysis included a total of 40 stringers and 37 frames. Each component is sized according to the structural analysis outputs (recall Table 8 and Table 11) and a skin thickness of 0.0403-in (18 gauge). The full CAD model is produced by transferring the structural analysis output to the CAD software, updating the components, and rebuilding the premade assembly (See Figure 18).

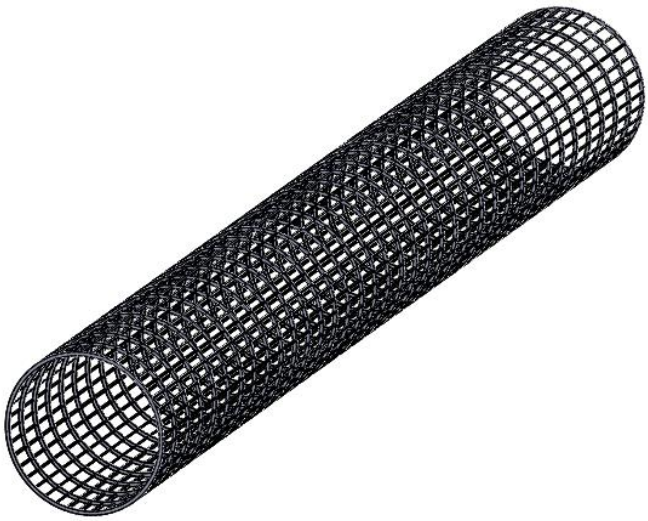

Figure 18. Business Jet: Full Fuselage Model without Skin

It is important to acknowledge the assumptions made to obtain this platform. First, the stringers and frames are assumed to be straight with constant cross section. In an actual aircraft fuselage, the diameter of the forward and aft frames decrease while the stringers gain curvature in accordance to the aerodynamic shape of the aircraft. Second, as previously discussed, this analysis does not account for longerons, skin doublers, etc. typically seen in modern aircraft. Finally, this analysis does not account for non-pressurized areas (such as the tail cone aft of the pressure bulkhead) and instead assumes the full fuselage is pressurized. These assumptions were made to simplify the overall analysis and ensure thesis completion. While this model does not account for the aerodynamic shape of the fuselage, it gives a good representation of the overall fuselage structure and provides a platform for FEA analysis.

FEA Verification

Using ANSYS an FEA analysis is conducted using the CAD model and applied loads. Due to the limitations of the software, and the large geometry, the CAD model is reduced to a single ring section (see Figure 19).

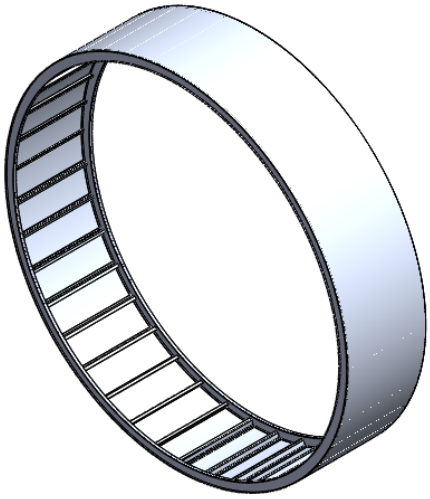

Figure 19. Business Jet: Single Fuselage Ring

This reduces the computational requirements of the FEA model and significantly reduces time required for each analysis. To ensure the entire structure is sized appropriately, the ring section corresponding to the wing junction (considered the worst case) is tested. By verifying the structural integrity of this section it is easy to justify the integrity of the entire structure.

After transferring the CAD geometry into the FEA software, the structure is meshed using the coarse mesh setting. Using this setting, ANSYS constructs a mesh containing 317,850 elements and 97,060 nodes (see Figure 20). While a finer mesh is possible, it significantly increases the required computation time, with little improvement in overall accuracy. Unfortunately, due to the size of the model any sort of convergence study froze the program.

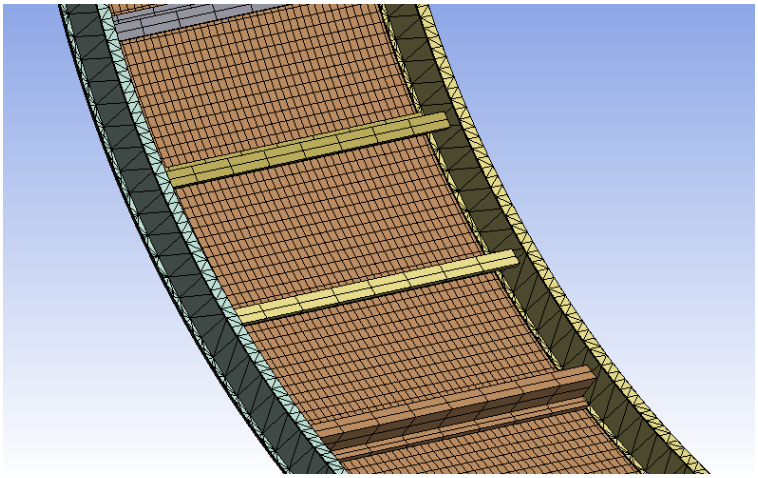

Figure 20. Business Jet: FEA Mesh

To verify the structural integrity under the applied pressure loads, the structure is fixed by the forward and aft frames and a 13.16-lbf/in^2 pressure is applied normal to the skin and stringers (recall Table 4). Next, an equivalent Von-Mises stress and total deformation analysis is conducted to verify the structural integrity. To pass this test, the structure may not exceed the material yield strength of 28,000-lbf/in^2 (Aluminum 2024-T3) for the skin and 46,000- lbf/in^2 (Aluminum 7075-T6) for the frames and stringers.

The equivalent Von-Mises stress analysis is arguably the most important analysis as it identifies whether or not the structure experiences stress above the required maximum yield strength. The results of the Von-Mises analysis can be seen in Figure 21.

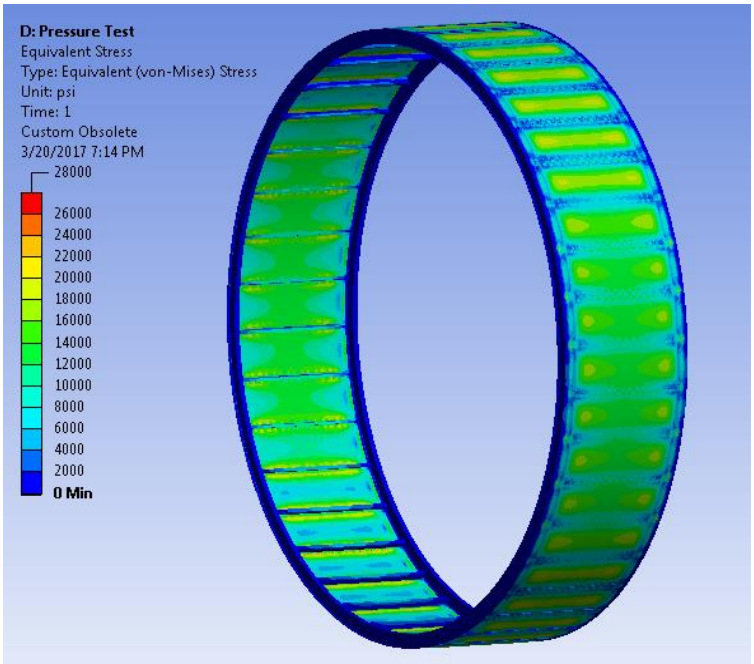

Figure 21. Business Jet: Von-Mises Stress Analysis (Pressure Test)

This analysis shows the structure to be well below the structural yield strength. The inner portions of the skin panels experience stress between 14,000-18,000-lbf/in^2, far below the 28,000-lbf/in^2 limit. The stringers also appear "cold" with the maximum stress between ~4,000-8,000-lbf/in^2, far below the 46,000-lbf/in^2 yield strength limit. Therefore, it is safe to say the structure is appropriately sized to withstand the applied pressure loads.

Next, a total deformation analysis is conducted to analyze the skin deflection under the applied pressure. The result of this analysis can be seen in Figure 22.

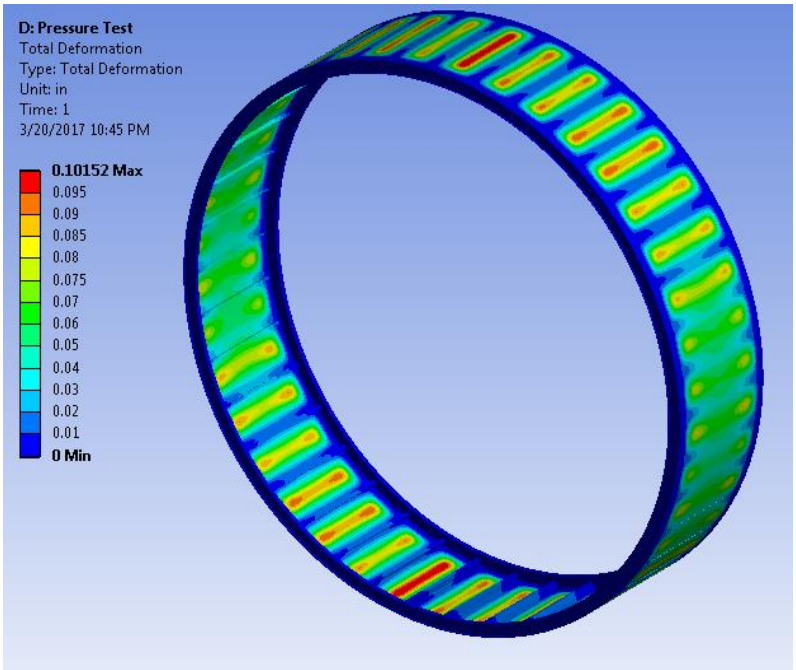

Figure 22. Business Jet: Deformation Analysis (Pressure Test)

This analysis shows a peak deformation of 0.10-in in the upper and lower section of the fuselage with the majority of the skin panels experiencing a deformation between 0.06-0.08-in.

Next, to verify the structural integrity of the fuselage under the applied flight loads, a full structural analysis is conducted applying the maximum shear and moment loads. To simulate this loading case, the structure is fixed by the aft frame representing the wing spar with the loads applied to the outer skin surface. This ensures the structure is allowed to deform and the loads are evenly distributed across the structure. The applied forces include a moment of 6,885,956-lbf-in and shear force of 34,229-lbf.

Similar to the pressure test, a Von-Mises analysis is conducted to ensure the stress acting on the fuselage remains below the material yield strength. If the stress is found to

be above these values, the structure is considered inadequate. The result of the Von-Mises stress analysis can be seen in Figure 23.

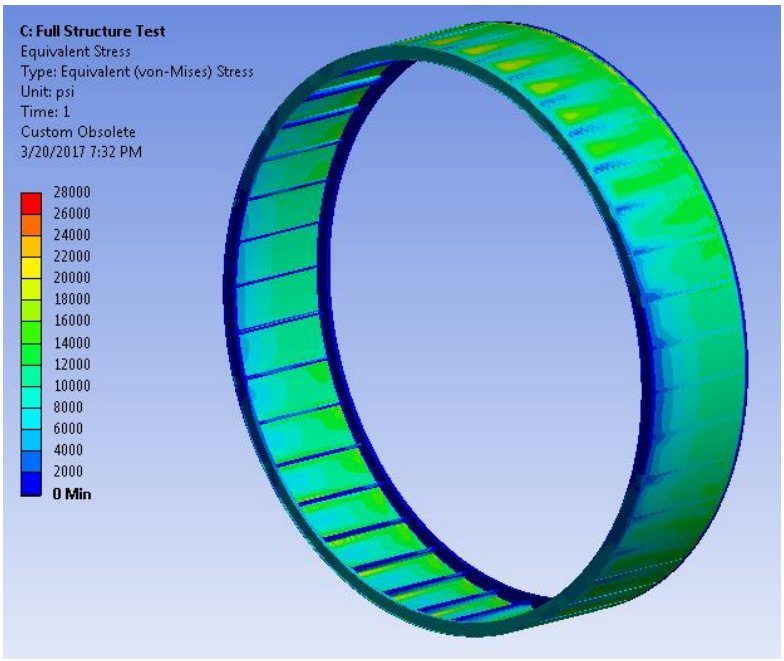

Figure 23. Business Jet: Full Von-Mises Stress Analysis (Isometric View)

Similar to the pressure test, the analysis shows the structure to be relatively "cool" with stress in the skin ranging from 12,000-20,000-lbf/in^2. This is well below the design yield strength of 28,000-lbf/in^2.

Looking closely at the stringers along the bottom of the fuselage (Figure 24), the stress is well below the 46,000-lbf/in^2 design limit with values between 2,000-18,000-lbf/in^2. At first glance it appears the stringers are oversized for the applied loads, thus resulting in the lower stress values. However, it is important to recall these components are sized based on the design buckling requirements. The stringers featured in Figure 24 have buckling strength limits of 16,038-lbf/in^2, slightly under the maximum stress. As would be expected, the stress increases at the frame and stringer intersection, creating a

slight stress concentration. This is partially due to the lack of adequate load path between the two components within the CAD model itself. In traditional structure, these components pass through the hoop frames and are connected using a shear clip. However, to simplify and reduce the geometry to a single frame section, the stringer stops coincident with the edge of the frame cap creating a stress singularity at this point. This in turn produces a “hot” spot at the lower corners of the stringers.

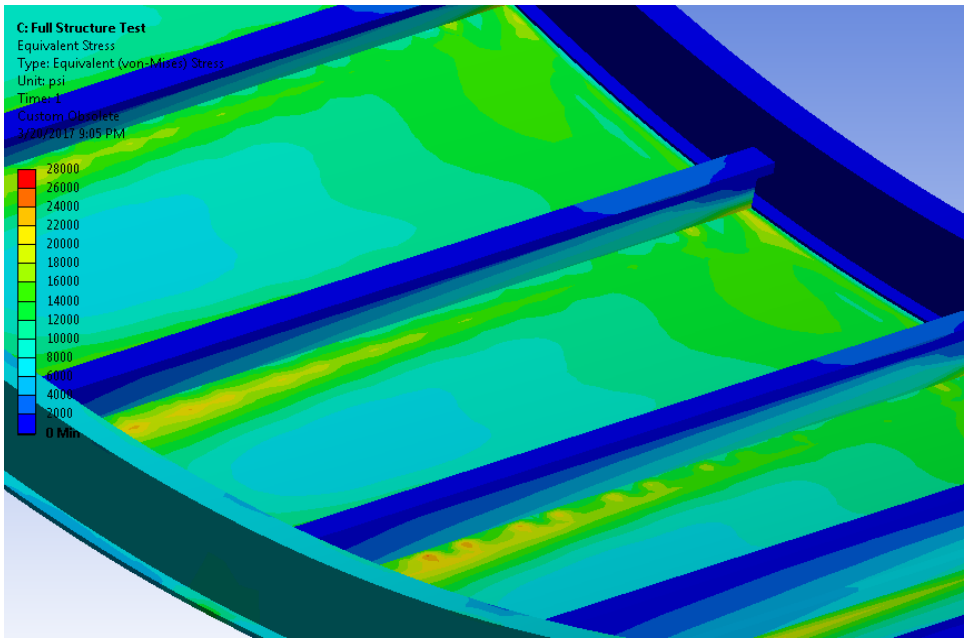

Figure 24. Business Jet: Full Von-Mises Stress Analysis (Lower Section)

Looking closely at the stringers in the middle of the fuselage (Figure 25), the Von-Mises stress is again well below the design yield strength with values ranging from 2,000-8,000-lbf/in^2. These components are sized for a buckling limit stress of 7,128-lbf/in^2. Similar to the lower stringers, the stress in the corners slightly exceeds this value due to the stress concentrations. While these hot spots certainly need to be addressed, the stress values are not high enough to raise any red flags.

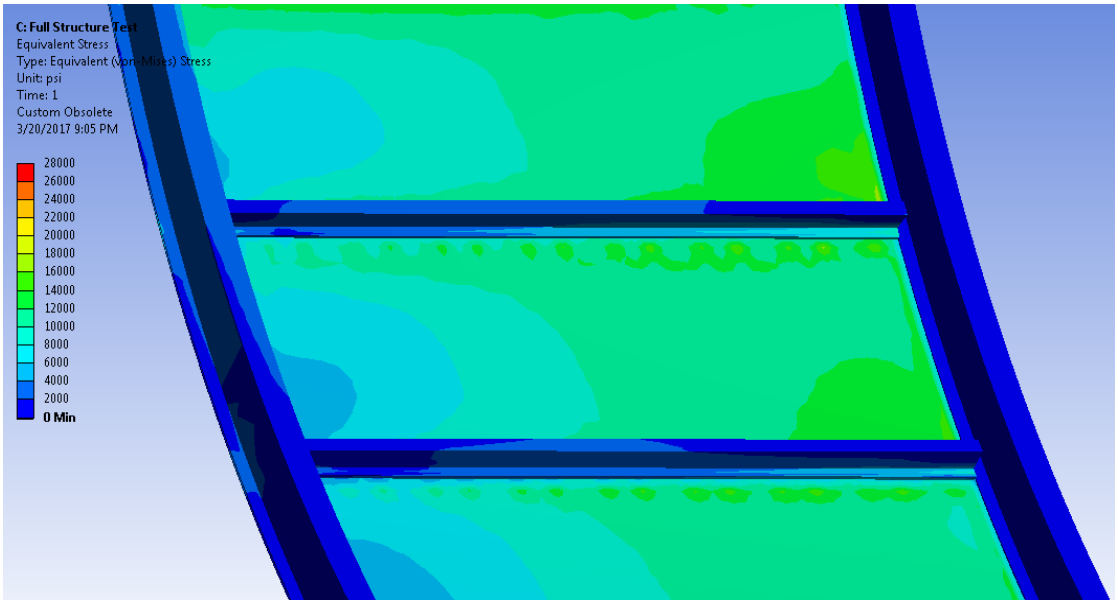

Figure 25. Business Jet: Full Von-Mises Stress Analysis (Mid-Section)

Looking back at Figure 24, the Von-Mises stress in the forward frame varies between 8,000-14,000-lbf/in^2. This is well under the design yield strength of 46,000-lbf/in^2. As previously explained, these components are oversized based on the prescribed sizing minimums. The frames have a minimum web height of 2-in to ensure adequate space for the stringers and future systems to pass through. In this analysis, all of the frame stations are sized based on this minimum sizing requirement.

To determine the deflection of the fuselage under the applied shear and moment loads, a deformation analysis is conducted (see Figure 26 and Figure 27).

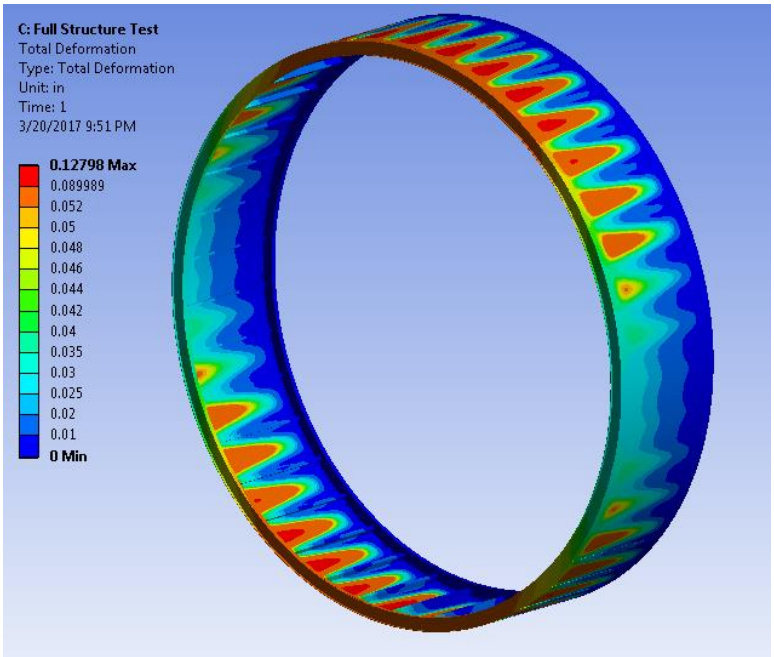

Figure 26. Business Jet: Full Deformation Analysis (Isometric View)

This analysis indicates the ring experiences a maximum deflection of 0.128-in along the upper and lower surfaces. Due to the large moment applied around the *y*-axis due to the applied tail loads, this result is expected. Extrapolating this result to the aft most ring section, assuming constant deflection across all sections, the tail deflects approximately 2.30-in under these loads.

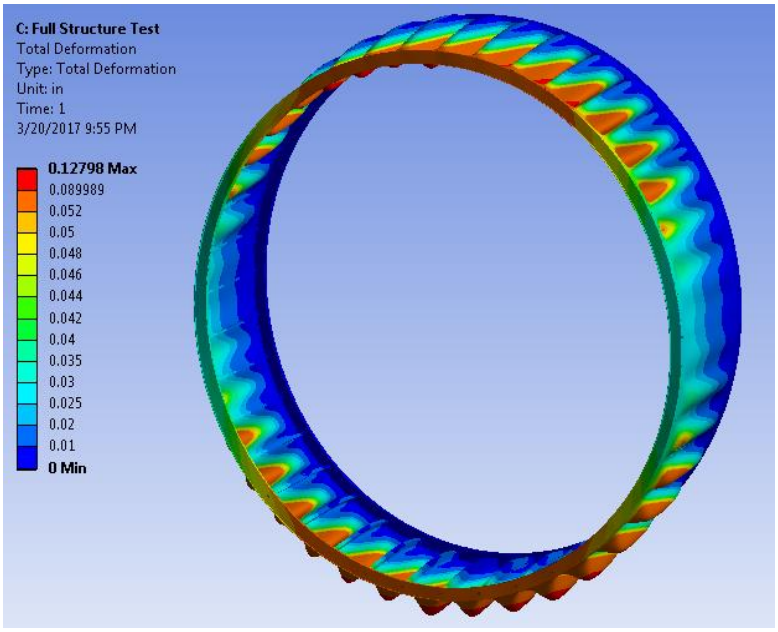

Figure 27. Business Jet: Full Deformation Analysis (Scaled x51)

Wide Body Commercial Jet Analysis

To test the program functionality on larger aircraft, an analysis based on "wide body" commercial airliners is conducted. Unlike the smaller business jet platform, this larger analysis does not rely on the minimum sizing thresholds within the program. Aircraft in the wide body category, such as the Boeing 777, Boeing 787, Airbus A330, etc., have fuselage diameters ranging from 18.5-ft (Boeing 787) up to 20-ft (Boeing 777).[18] These aircraft are also much longer, stretching upwards of 200-ft, and capable of taking off with an MTOW approaching 800,000-lbm.

Design Inputs

Similar to the previous analysis, the first step in the process is to supply the program with all of the design variables. These inputs, again, include basic fuselage dimensions, cabin and cruising altitude, estimated point masses, and anticipated tail and landing loads. These parameters are largely based on aircraft data found in Niu's design handbook[18] and published data on wide body aircraft.[28]

Wide body commercial airliners have fuselage diameters ranging from 18.5-ft to 20-ft and stretch over 200-ft, so a 209-ft long fuselage with a 20-ft diameter is used in this analysis. Similar to the business jet analysis, the stringer and frame spacing is set to 7-in and 20-in respectively. This spacing results in 108 stringers equally spaced around the diameter of the fuselage, and 125 equally spaced frame stations. This sizing data is based off of published data on the Boeing 777[28] and Niu's tabulated data on aircraft sizing.[18] A complete list of basic sizing inputs can be seen in Table 13.

Table 13. Wide Body: Sizing Inputs

Fuselage	
Length	2,509 in
Diameter	244 in
Frame Spacing	20 in
Number of Stringers	108
Wing Spar Location	1,200 in
Est. Structural Weight	140,000 lbm

Next, the internal cabin pressure is set based on the cabin altitude and desired cruising altitude. Aircraft in this category typically have cabin altitudes of ~8,000-ft and service ceilings around 40,000-ft. Therefore, a cabin altitude of 8,000-ft and service altitude of 43,000-ft is used for this analysis. Using the standard atmosphere table the

positive and negative pressurization loads are calculated to be 8.80-lbf/in^2 and -0.5-lbf/in^2 respectively. The aircraft's service ceiling is set below 45,000-ft, so a 1.33 factor of safety is applied to the previously calculated pressurization loads. Applying this factor, the design positive pressurization load is calculated to be 11.71-lbf/in^2 while the negative pressurization load is calculated to be -0.665-lbf/in^2. This pressure load is applied to the internal structure creating tension stress on the internal fuselage components.

The aircraft flight loads are again based on 14 CFR § 25.337 (b) and (c) [27] and an estimated MTOW of 766,000-lbm. According to 14 CFR § 25.337 (b), [27] this results in the minimum +2.5-g flight load applied to the airframe.

Due to the size of this aircraft, the tail and landing loads play a large role in the structural sizing. Again, the approximate tail load is based on the aircraft dimensions, and anticipated flight conditions. For the purpose of this analysis, the dynamic pressure is calculated based on an estimated maximum dive speed of 400-KIAS and altitude of 10,000-ft. Again, this is based off on a simulated rapid decompression scenario where the aircraft is forced to dive to 10,000-ft as quickly as possible. Using a standard atmosphere table, the dynamic pressure is calculated to be 543-lbf/ft^2. The aircraft is assumed to have a wing reference area of 4,605-ft^2, a wing mean geometric chord of 23-ft, and tail moment arm of 85-ft (based on the tail and wing spar locations). Using these parameters the horizontal trim load is calculated to be 182,685-lbf to trim a +2.5-g pull up at maximum dynamic pressure (400 KIAS). Again, this assumes the aircraft's CG location renders it 35% stable. A summary of estimated flight, tail, and landing loads can be seen in Table 14.

Table 14. Wide Body: Applied Loads

Flight	
Flight Load	+2.5 g
Landing	
Nose Gear	50,000 lbf
Tail	
Horizontal	182,685 lbf
Pressure	
Positive	11.707 lbf/in^2
Negative	-0.665 lbf/in^2

The final primary force comes from the point mass loads. These loads include a combination of published weights, empirically estimated weights, and approximate component weights. Aircraft in this category typically have large seating capacities with some carrying over 300 passengers. This analysis estimates an international passenger load of 237 basic economy passengers and 42 first class passengers. The approximate weights include two pilots estimated at 175-lbm each, cockpit furnishing estimated at 500-lbm, two galleys estimated at 1,500-lbm, and six lavatories estimated at 500-lbm. A complete list of the applied point mass loads along with their respective locations can be seen in Table 15.

Table 15. Wide Body: Point Masses

Component	Location Start (in)	Location End (in)	Weight (lbm)
Avionics	12	60	6,050
Cockpit Furnishing	60	120	500
Pilots	72	96	350
Passenger Furnishing	300	1,950	12,630
Payload	300	2,100	78,335
APU	2,437	2,509	1,100
Forward Lavatory	120	180	1,000
Mid Lavatory	1,000	1,060	1,000
Aft Lavatory	1,950	2,010	1,000
Nose Gear	232	244	3,950
Vertical Tail	1,950	2,330	5,980
Horizontal Tail	2,100	2,340	8,034
Forward Galley	120	300	1,500
Aft Galley	1,950	2,130	1,500

Similar to the previous analysis, Aluminum 2024-T3 is used for the skin and Aluminum 7075-T6 is used for the frames and stringers. A summary of the materials used for each component can be seen in Table 16.

Table 16. Wide Body: Material Choices

Material	
Skin	Aluminum 2024-T3
Stringer	Aluminum 7075-T6
Frame	Aluminum 7075-T6

Program Outputs

The program utilizes the user supplied inputs to design and size a conceptual wide body fuselage. First, the program calculates the preliminary skin thickness based on the desired cabin altitude and fuselage radius supplied by the user. Using these values, the program calculates the hoop stress and compares this value with the material strength characteristics. If the calculated stress is above the material yield strength, taking into account the appropriate factors of safety, the skin thickness is increased and the process repeats. In this analysis, the skin has a maximum yield strength of 42,000-lbf/in^2, which is de-rated to 28,000-lbf/in^2 after applying the 1.5 FOS. Starting with the minimum gauge skin thickness of 0.032-in (20 gauge) the program calculates the necessary skin thickness as follows:

$$F_{Hoop} = \frac{(11.71\, lbf/in^2\,)(122in)}{0.032in} = 44{,}606\, lbf/in^2$$

$$F_{Design} = \frac{42{,}000\, lbf/in^2}{1.5} = 28{,}000\, lbf/in^2$$

$$F_{Hoop} > F_{Design} \rightarrow T_{skin} = 0.0403in$$

$$F_{Hoop} = \frac{(11.707\, lbf/in^2\,)(122in)}{0.0403in} = 35{,}441\, \frac{lbf}{in^2}$$

$$F_{Hoop} > F_{Design} \rightarrow T_{skin} = 0.0508in$$

$$F_{Hoop} = \frac{(11.707\, lbf/in^2\,)(122in)}{0.0508in} = 28{,}115\, \frac{lbf}{in^2}$$

$$F_{Hoop} > F_{Design} \rightarrow T_{skin} = 0.0641in$$

$$F_{Hoop} = \frac{(11.707\, lbf/in^2\,)(122in)}{0.0641in} = 22{,}282\, \frac{lbf}{in^2}$$

$$F_{Hoop} < F_{Design} \rightarrow T_{skin} = 0.0641in$$

From this analysis, the initial skin thickness is set to 0.0641-in (14 gauge).

Next, using the previously calculated skin thickness, the program calculates the panel buckling forces. Utilizing the frame and stringer spacing of 20-in and ~7-in respectively, the program interpolates the shear and buckling coefficients (recall Figure 6 and Figure 7). These coefficients, along with the material characteristics, are used to calculate the maximum allowable force on the skin (see Table 17).

Table 17. Wide Body: Initial Panel Buckling Strength

Type	Coefficient	Strength (lbf/in^2)
Compression	3.60	3,083
Shear	7.46	6,390

These values are stored and used to verify the fuselage skin thickness later on in the analysis.

To size the frames the program first calculates the shear and moments acting on each individual frame station. Using the overall fuselage length and frame spacing, the fuselage is divided into 125 frame stations with 60 forward of the wing spar and 65 aft. Next, the program creates a lumped mass model based on the user defined point masses. These loads are evenly distributed throughout the fuselage and multiplied by the positive flight load, previously calculated to be 2.5. The lumped mass models for the forward and aft sections of the fuselage can be seen in Figure 28 and Figure 29.

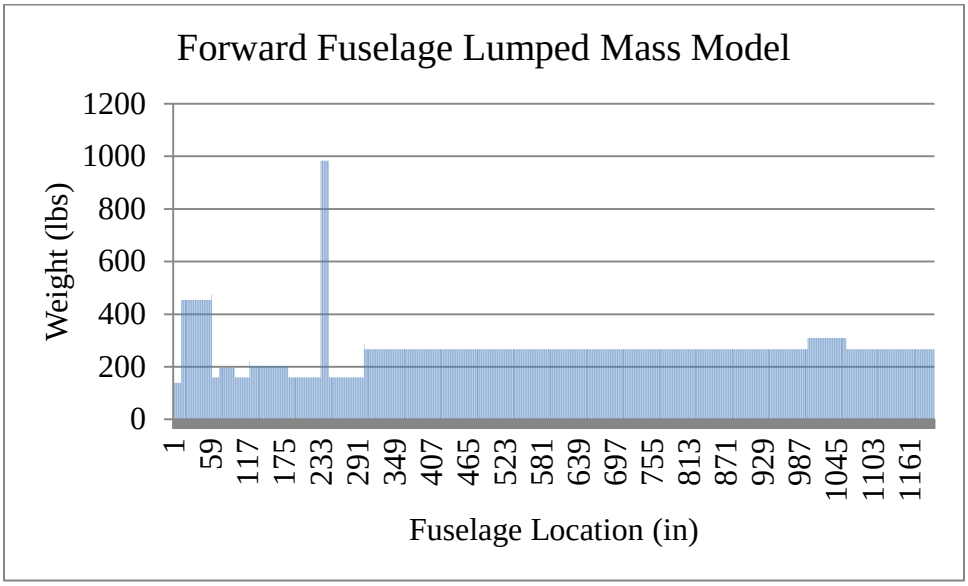

Figure 28. Wide Body: Forward Fuselage Lumped Mass Model

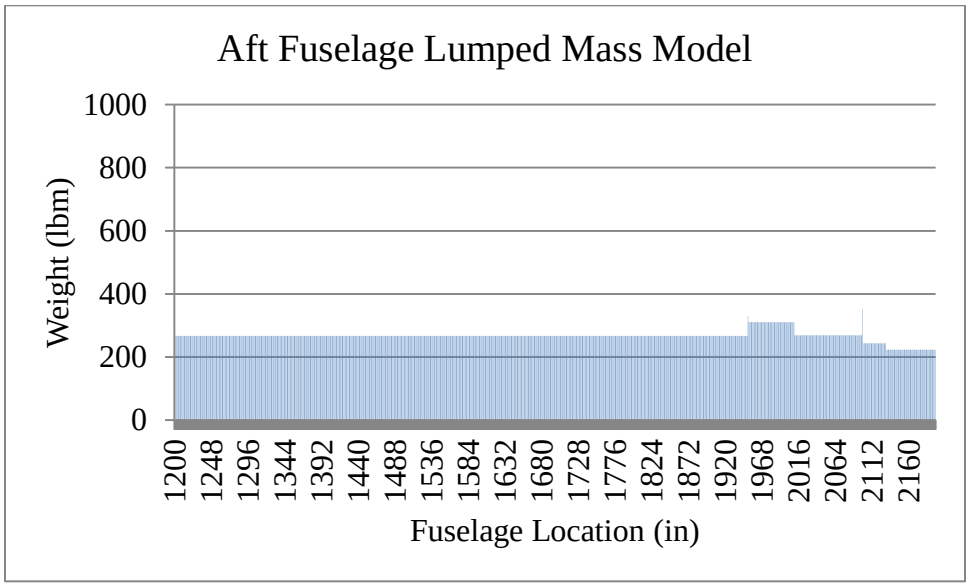

Figure 29. Wide Body: Aft Fuselage Lumped Mass Model

Similar to the previous analysis, this lumped mass model is used to create shear and moment buildups for the entire fuselage. Starting at the nose of the fuselage moving aft, the program integrates the applied loads up to the wing spar. This creates a shear build up for the forward section of the fuselage with a maximum shear force of 373,880-

lbf. Next, starting at the tail of the aircraft moving forward, the program repeats the process by integrating the applied loads until it reaches the wing spar. This creates a shear build up for the aft portion of the fuselage with a maximum shear force of 507,857-lbf at the wing spar (see Figure 30)

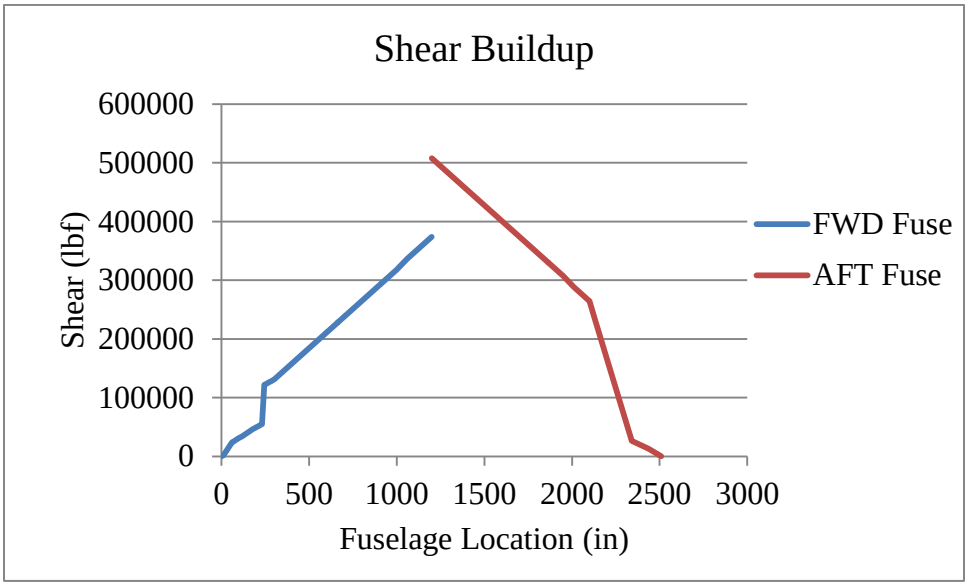

Figure 30. Wide Body: Shear Buildup

A similar integration method is used to calculate the moment buildup. In this case the shear force is integrated starting at the nose or tail and moving towards the wing spar. Due to the applied tail loads far outweighing the landing loads, the aft section of the fuselage experiences a greater force. The maximum moment in the forward section of the fuselage is calculated to be 242,000,000-lbf-in^2 and 386,000,000-lbf-in^2 in the aft. The moment build up for each section can be seen in Figure 31 .

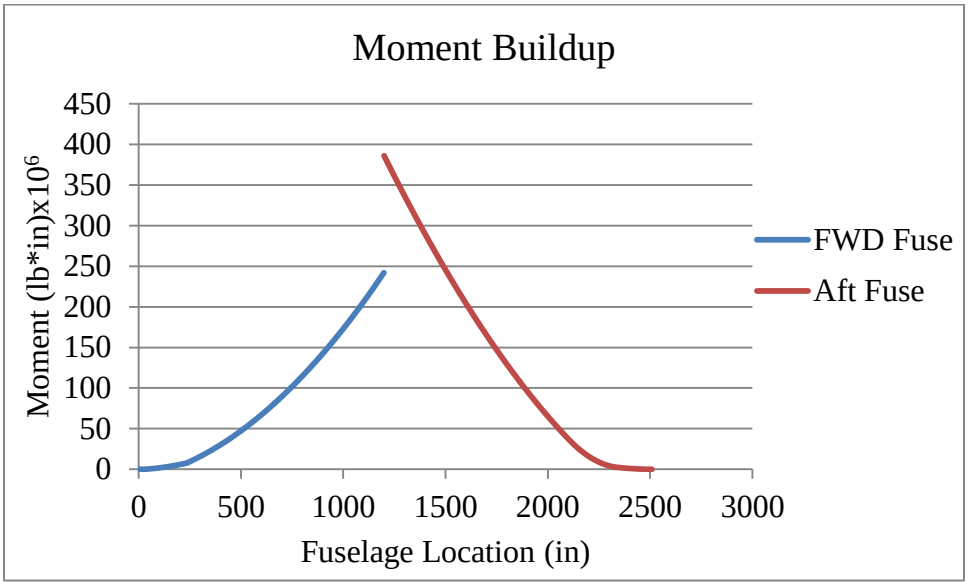

Figure 31. Wide Body: Moment Buildup

Again, this analysis assumes the aircraft is "fixed" at the wing spar location creating a discontinuity between the forward and aft fuselage sections. The tail loads, in this case, far outweigh the landing loads resulting in a higher force applied to the aft fuselage, as seen in Figure 30 and 31. This discontinuity is not seen in actual aircraft as the load path is continuous; however, this analysis cannot be conducted without fixing the aircraft at some point.

Next, the program utilizes the data collected from the shear and moment buildups to calculate the required area moment of inertia for each frame station. This value is used to search through a list of possible frame sizes until an optimal size is found. Unlike the previous analysis, most of the frames do not depend on the minimum sizing requirements. The loads in this analysis are large enough to create variation in the overall frame sizing. As would be expected, the largest area moment of inertia is calculated at the wing spar resulting in the largest relative frame size at this location. The smallest frames,

on the other hand, are located towards the front and back of the fuselage where the applied moment is lowest. In this case, the load is not large enough to move the size off of the predefined minimum. Starting at the nose of the fuselage, the frames are sized to the minimum frame limit until the 12^{th} frame station at which point the frame thickness increases a single gauge (14 to 12 gauge). The frame sizing continues to grow as it approaches the wing spar before decreasing back to the minimum frame sizing near the tail. The dimensions for all 125 frame stations can be seen in Table 21 located in the appendix.

The final step in the analysis is the stringer sizing. This process takes into account the shear and moment buildups and basic aircraft geometry to build an extensive shear build up to size the stringers. Starting with the minimum stringer sizing, the program calculates the shear and compressive loads on the stringers and skin and compares these values to the buckling, crippling, and material strength limits. If the stringer sizing is found to be inadequate, the program increases the sizing, moves to the remaining stringers, and starts over. The shear force acting on each stringer is dependent on the stringer next to it creating a rippling effect as the sizing changes. Therefore, the process is repeated multiple times to ensure each stringer is optimally sized. A sample shear build up for the worst shear case can be found Table 22 located in the appendix.

Again, due to symmetry only 28 of the 108 stringers are analyzed with the results mirrored across the *x* and *z* axis. Each stringer is sized based on either the design material strength or the crippling and buckling strength found in Table 18.

Table 18. Wide Body: Stringer Strength Values

Stringer #	Crippling Strength (lbf/in^2)	Buckling Strength (lbf/in^2)
1|55	265,218	96,229
2|54|56|40|108	265,218	96,229
3|53|57|39|107	265,218	96,229
4|52|58|38|106	265,218	96,229
5|51|59|37|105	265,218	96,229
6|50|60|36|104	265,218	96,229
7|49|61|35|103	289,713	96,229
8|48|62|34|102	289,713	96,229
9|47|63|33|101	289,713	96,229
10|46|64|32|100	289,713	96,229
11|45|65|99	289,713	96,229
12|44|66|98	289,713	96,229
13|43|67|97	289,713	96,229
14|42|68|96	289,713	96,229
15|41|69|95	297,992	96,229
16|40|70|94	297,992	66,825
17|39|71|93	297,992	66,825
18|38|72|92	297,992	66,825
19|37|73|91	297,992	66,825
20|36|74|90	297,992	66,825
21|35|75|89	297,992	66,825
22|34|76|88	297,992	66,825
23|33|77|87	297,992	66,825
24|32|78|86	501,160	66,825
25|31|79|85	501,160	42,768
26|30|80|84	501,160	42,768
27|29|81|83	501,160	42,768
28|82	501,160	42,768

From this analysis, and the results shown in Table 22 located in the appendix, it is clear the stringers are sized based on a combination of buckling and material yield strength. The majority of the stringers have buckling strength limits well above the material yield strength. Therefore, the compressive force must be held below the material

yield strength to prevent structural failure. As the analysis moves towards the left and right halves of the fuselage, the stringers return to buckling dominated sizing as the buckling strength is less than the material yield strength. Again, these components are not crippling dominated components as the design crippling strength is far greater than the design buckling strength. The program continues through each frame station storing the sizing for each individual stringer. After the final frame station has been analyzed, the program outputs the stored stringer sizes. A table displaying all stringer dimensions can be seen in Table 19.

Table 19. Wide Body: Stringer Dimensions

Stringer #	Cap Width (in)	Web Height (in)	Thickness (in)
1|55	0.625	1.25	0.375
2|54|56|40|108	0.625	1.25	0.375
3|53|57|39|107	0.625	1.25	0.25
4|52|58|38|106	0.625	1.25	0.25
5|51|59|37|105	0.625	1.25	0.25
6|50|60|36|104	0.625	1.25	0.25
7|49|61|35|103	0.625	1.25	0.25
8|48|62|34|102	0.625	1.25	0.25
9|47|63|33|101	0.625	1.25	0.25
10|46|64|32|100	0.625	1.25	0.25
11|45|65|99	0.625	1.25	0.25
12|44|66|98	0.625	1.25	0.25
13|43|67|97	0.625	1.25	0.25
14|42|68|96	0.625	1.00	0.25
15|41|69|95	0.625	1.00	0.25
16|40|70|94	0.625	1.00	0.25
17|39|71|93	0.625	1.00	0.25
18|38|72|92	0.625	1.00	0.25
19|37|73|91	0.625	1.00	0.25
20|36|74|90	0.625	1.00	0.25
21|35|75|89	0.50	1.00	0.25
22|34|76|88	0.50	1.00	0.25
23|33|77|87	0.50	1.00	0.25
24|32|78|86	0.50	1.00	0.25
25|31|79|85	0.375	0.75	0.25
26|30|80|84	0.375	0.75	0.25
27|29|81|83	0.375	0.75	0.25
28|82	0.375	0.75	0.25

During this process the program also revisits the skin thickness as it progresses through the shear build up. This ensures the skin, previously sized for pressure loads, is adequate for the applied shear loads. If the shear force exceeds the stiffened panel buckling criteria (recall Table 17) the skin thickness is increased, and the process repeats.

In this case the program found the skin thickness (previously set to 0.0641-in based on pressure loads) to be inadequate and resized the skin to 0.0808-in thick (12 gauge). This results in the new panel buckling criteria seen in Table 20.

Table 20. Wide Body: Final Panel Buckling Strength

Type	Coefficient	Strength (lbf/in^2)
Compression	3.60	4,899
Shear	7.27	9,898

Again, it is important to keep in mind the skin sizing is based on the worst shear case which occurs near the wing spar. The majority of the fuselage skin is sized purely off of the pressurization loads as the shear stress does not exceed the shear buckling limits. Therefore, skin doublers can be implemented near the wing spar to effectively thicken the skin, leaving the rest of the fuselage skin at the previously found 0.0641-in (14 gauge) thickness.

At the conclusion of the structural analysis process the program outputs the sizing for each component. These dimensions are transferred to the parameterized CAD model and used to model the full fuselage structure.

CAD Geometry

Again, the CAD model is split into four parameterized components: the skin, frames, stringers, and full assembly. Each component is parameterized to accept the dimensions found in the structural analysis tool. Using the new dimensions the model automatically resizes to represent the new geometry. An example of a parameterized *I*-frame can be seen in Figure 32.

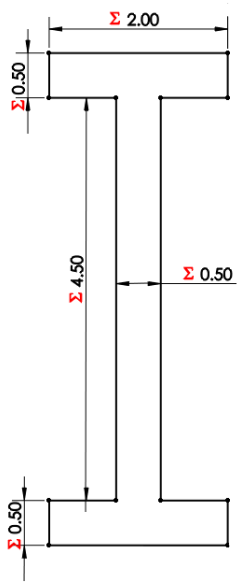

Figure 32. Parameterized *I*-Frame

This component, similar to the stringer setup shown in the previous analysis, is setup to accept web height, cap width, and material thickness.

This analysis featured a total of 108 stringers and 125 frames. Each component is sized according to the structural analysis outputs (recall Table 19 and Table 21) and a skin thickness of 0.0808-in. The full CAD model can be seen in Figure 33.

Figure 33. Wide Body: Full Fuselage Model without Skin

Similar to the previous analysis, this model does not take into account the aerodynamic shape of the fuselage or additional structural components not included in the structural analysis tool. This model gives a good representation of the overall size and shape of the fuselage and provides a platform for further FEA analysis.

FEA Verification

To verify the structural sizing, an FEA analysis is conducted using the CAD model and applied loads. Again, due to the limitations of the FEA software, the CAD model is reduced to a single ring section (see Figure 34)

Figure 34. Wide Body: Single Fuselage Ring

Similar to the previous analysis, this ring corresponds to the wing junction which experiences the worst loading case. Verifying the structural integrity of this ring justifies the sizing of the remaining structure.

After transferring the CAD model into the FEA software, the structure is meshed using a coarse mesh. This setting creates a mesh consisting of 249,798 elements and

82,046 nodes (see Figure 35). Again, while a finer mesh is possible, it significantly impacts the computation time. In an effort to keep the model size to a minimum without sacrificing accuracy, the coarse mesh is considered adequate for this analysis.

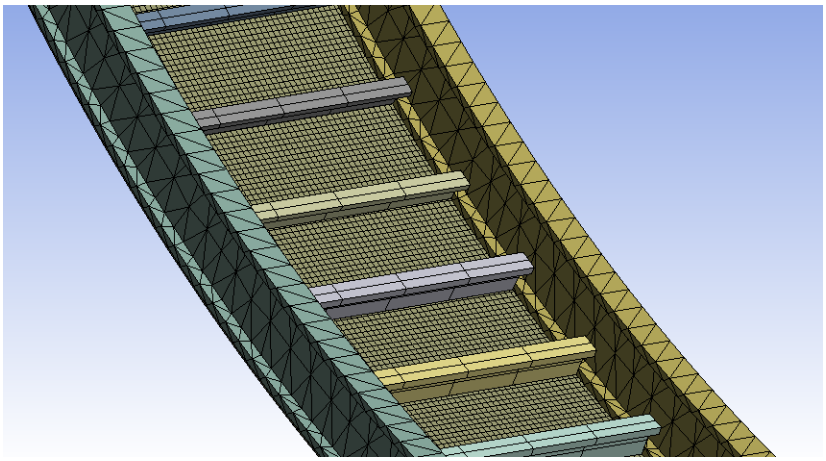

Figure 35. Wide Body: FEA Mesh

To verify the structural integrity under the applied pressure loads, the structure is fixed by the forward and aft frames and an 11.707-lbf/in^2 pressure is applied to the skin and stringers (recall Table 14). To pass the test, the structure cannot exceed the material yield strength of 28,000-lbf/in^2 (Aluminum 2024-T3) for the skin and 46,000-lbf/in^2 (Aluminum 7075-T6) for the frames and stringers. Using a static structural analysis, the equivalent Von-Mises stress and total deformation is analyzed based on the applied pressure load.

The Von-Mises stress analysis is especially useful as it determines whether or not the structure experiences stress above the design yield strength. The Von-Mises results for the simple pressure case can be seen in Figure 36.

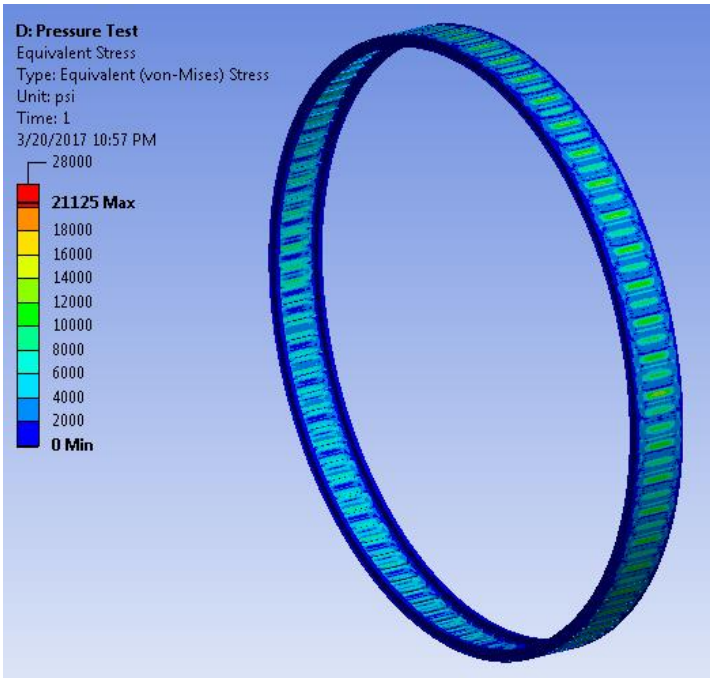

Figure 36. Wide Body: Von-Mises Stress Analysis (Pressure Case-Isometric)

This analysis shows the structure to be relatively "cold" throughout. The majority of the skin has stress between 8,000-12,000-lbf/in^2 which is well below the 28,000-lbf/in^2 material limits. Taking a closer look at the inner skin panels (see Figure 37) it is clear the stringers are also "cold" with Von-Mises stress values between 6,000-10,000-lbf/in^2.

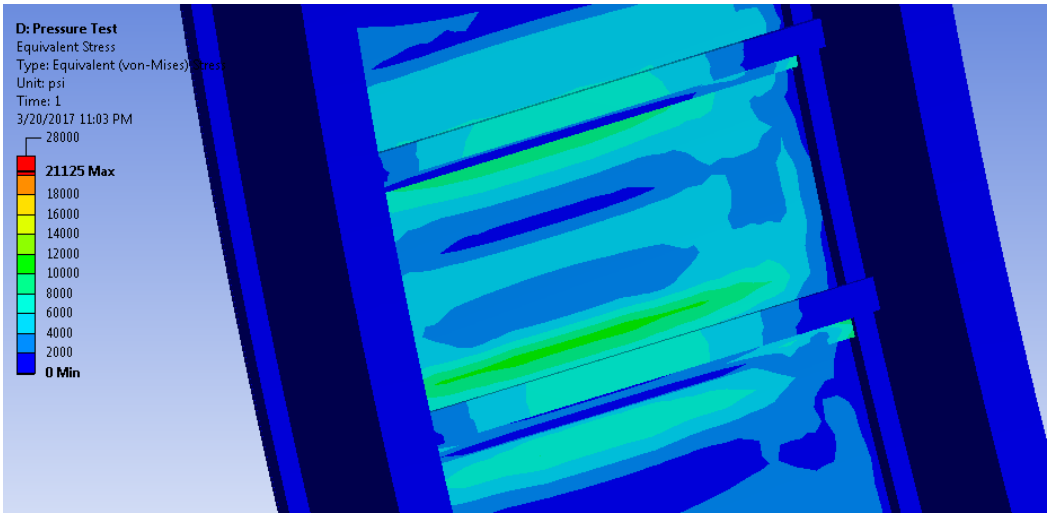

Figure 37. Wide Body: Von-Mises Stress Analysis (Pressure Case-Inner Surface)

With all Von-Mises stress values well below the material limits, it is safe to say the structure is appropriately sized to withstand the applied pressure loads.

To further investigate how far the skin stretches under the applied pressure loads, a total deformation analysis is conducted (see Figure 38). This analysis shows a maximum deflection of 0.08-in along the left and right sides of the fuselage with the majority of the fuselage stretching between 0.04-0.07-in.

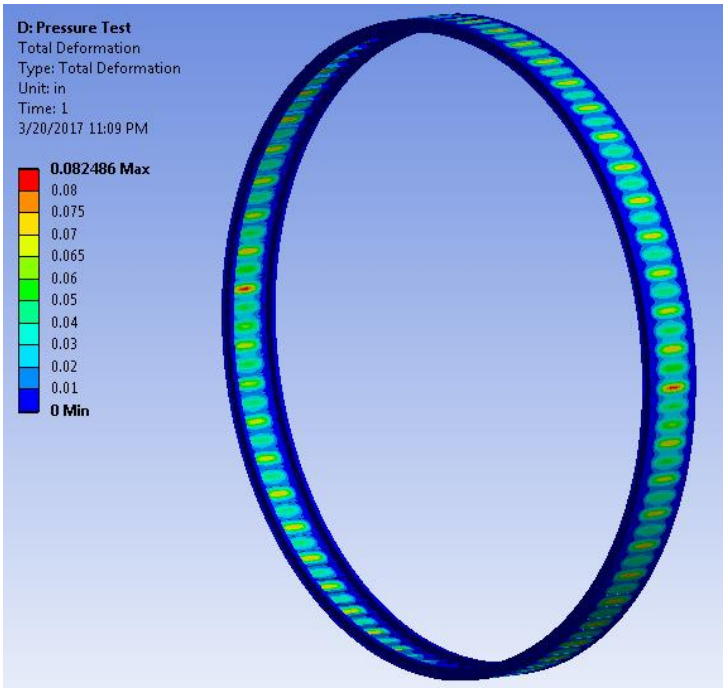

Figure 38. Wide Body: Total Deformation Analysis (Pressure Case)

From the results shown in Figure 36-38, it is clear the structure is adequately sized for the applied pressure loads.

The next, and most important analysis, is conducted with both shear and moment loads (corresponding to the wing junction) acting on the structure. It is important to note that the pressure loads are not applied in this analysis. This is due to the design case simulating a high speed dive to 10,000-ft followed by a +2.5-g pull up. Under these conditions the pressurization load is almost negligible, and thus left out of the analysis. To simulate the loading case, the structure is fixed by the aft frame representing the wing spar location. In order to evenly distribute the loads across the entire structure, the applied moment of 386,000,000-lbf-in is applied to the outer skin surface. The skin is connected to all of the components enabling a continuous load path to the entire structure. The maximum shear force of 507,857-lbf is applied to the structure via remote force. This

allows the force to be applied from the center point of the ring structure in the negative z-direction. After the boundary conditions are set the FEA software is used to analyze the resulting Von-Mises stress on the structure.

Similar to the pressure test, the Von-Mises analysis is conducted to ensure the stress acting on the fuselage structure remains below the material yield strength. If the stress is found to be above these values, the structure is considered inadequate. The result of the Von-Mises stress analysis can be seen in Figure 39.

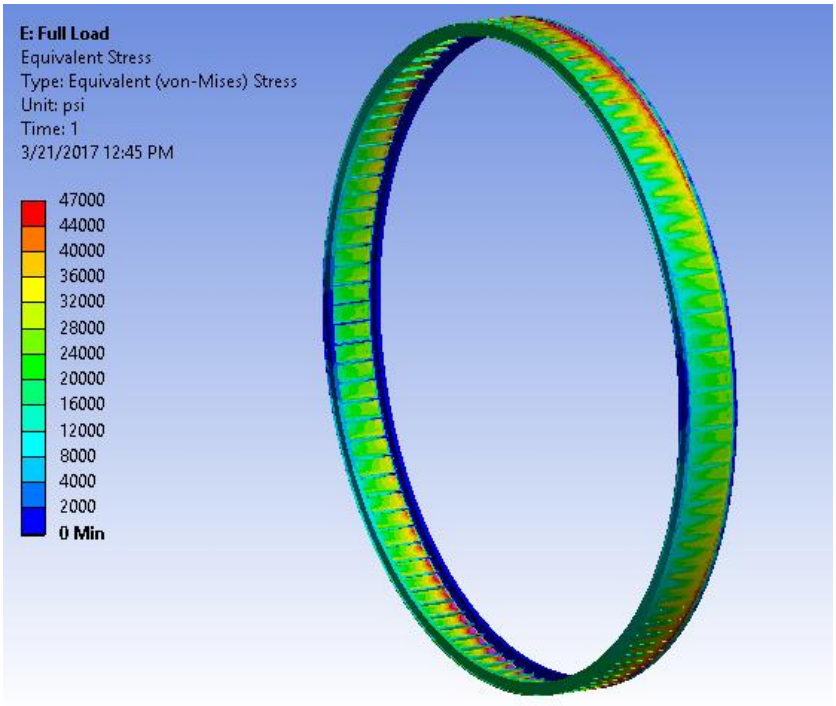

Figure 39. Wide Body: Full Von-Mises Stress Analysis (Isometric View)

Unfortunately, these results show the skin is not sized to withstand the applied moment and shear loads. The majority of the skin experiences Von-Mises stress above the design yield strength of the material (28,000-lbf/in^2) with areas near the top and bottom of the ring exceeding the material yield strength of 42,000-lbf/in^2. This result is likely due to the increased load created by "fixing" the fuselage at the wing spar. In

reality, this load is less severe in flight; however, this program is designed to size the skin correctly for the applied loads regardless of their severity. Therefore, as a result of this analysis, a crippling factor is added to the skin sizing with the results shown in the next section.

Looking closely at the frames and stringers (see Figure 40), all components appear under the design yield strength for Aluminum 7075-T6 (46,000-lbf/in^2) and under the buckling requirements set forth for the stringers. It is important to remember the stringers featured in Figure 40 are sized based on the design yield strength and not the buckling criteria. In this case the buckling strength is well above the design yield strength, making the stringers in this section strength dominated. The highest stress in these components is again located near the frame and stringer intersection. As explained in the previous analysis, these intersections create stress concentrations due to the inadequate load path between components. However, the stress in these areas is still below the design yield strength of the material.

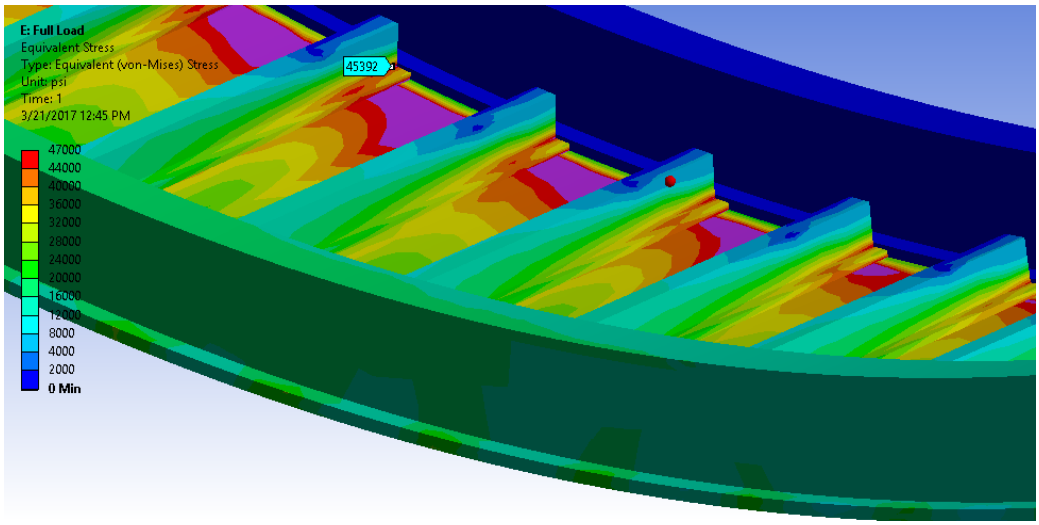

Figure 40. Wide Body: Full Von-Mises Stress Analysis (Lower Section)

Moving around the fuselage to the mid-section, Figure 41 shows the stringers are adequately sized in this area. The four stringers featured in Figure 41 are buckling dominated components with a maximum buckling strength of 42,768-lbf/in^2. This analysis shows Von-Mises stress values between 4,000-18,000-lbf/in^2 which again, is well below the strength requirements.

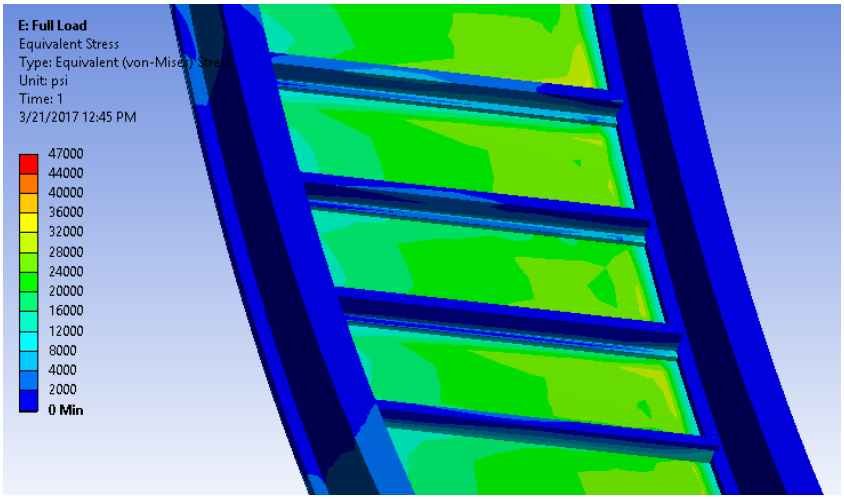

Figure 41. Wide Body: Full Von-Mises Stress Analysis (Mid-Section)

The frames, on the other hand, have Von-Mises stress between 16,000-28,000-lbf/in^2 which is well below the design yield strength. Therefore, based on the results shown in Figure 40 and Figure 41 a crippling factor is not needed for the frames and stringers.

Crippling Factor

Based on the FEA results in the Wide Body analysis, a crippling factor is added to the skin sizing algorithm. This crippling factor accounts for the fact the design algorithm decomposes a 3D stress problem into a set of 1D stress problems, only one of which ultimately controls structural sizing. This inaccuracy shows up in the wide body Von-

Mises stress analysis which shows the skin to be under sized for the applied loads. To account for this, a 40% crippling factor is applied to the skin thickness and the business jet and wide body FEA analysis are repeated to ensure the crippling factor is sufficient.

Using the new crippling factor the business jet is reproduced with 0.0564-in thick skin. This modification is made within the CAD model and the ANSYS Von-Mises stress analysis is repeated with the results shown in Figure 42.

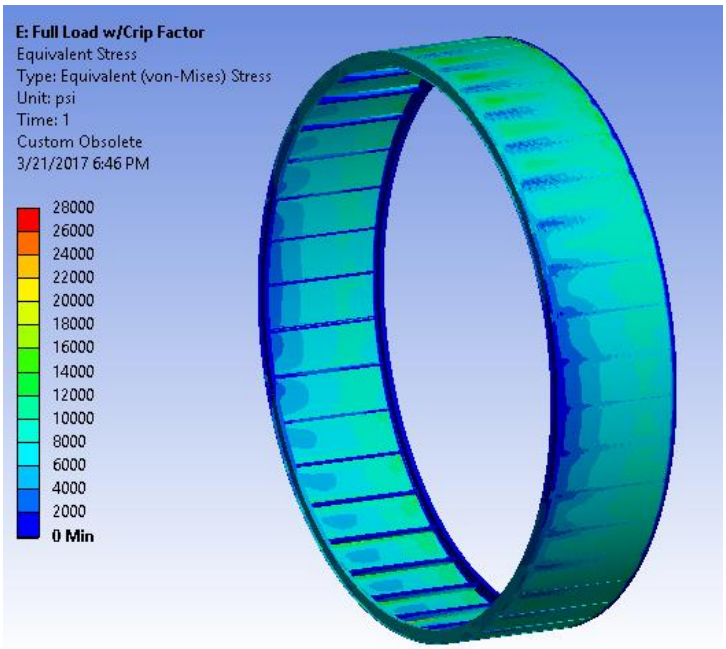

Figure 42. Business Jet: Von-Mises Stress Analysis with Crippling Factor (Isometric)

From these results the Von-Mises stress is still well below the material limits. This result was expected, but the analysis was repeated for consistency. The pressure and total deformation tests are left out of the analysis as the business jet already passed the analysis with the original skin thickness.

Applying the crippling factor to the Wide Body structure, the skin thickness increases from the previous 0.080-in thickness to 0.113-in. This modification is made

within the CAD model and the ANSYS Von-Mises stress, along with the total deformation analysis, is repeated with the results shown in Figure 43 and Figure 44.

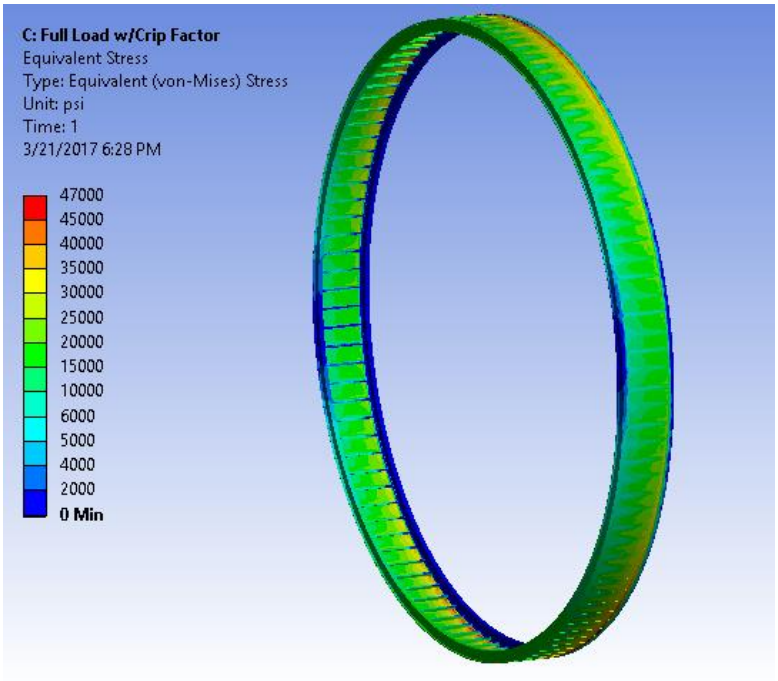

Figure 43. Wide Body: Von-Mises Stress Analysis with Crippling Factor (Isometric)

The Von-Mises stress analysis (Figure 43) indicates a significant decrease with the thickened skin. The majority of the fuselage skin is below the design yield strength (28,000-lbf/in^2) with Von-Mises stress values ranging from 15,000-25,000-lbf/in^2. Looking closely at the upper and lower sections of the ring, a small section near the frame intersection exceeds the design yield strength with values ranging from 30,000-40,000-lbf/in^2. These "hot spots" are attributed to the stress concentration created by the skin and frame intersection. While these "hot spots" are troubling, the stress is right around the material yield strength, and with the assumptions made during this analysis increasing the overall load, the crippling factor is considered adequate for use in this

design tool. The frames and stringers, again, are well below the design yield strength for Aluminum 7075 (46,000-lbf/in^2).

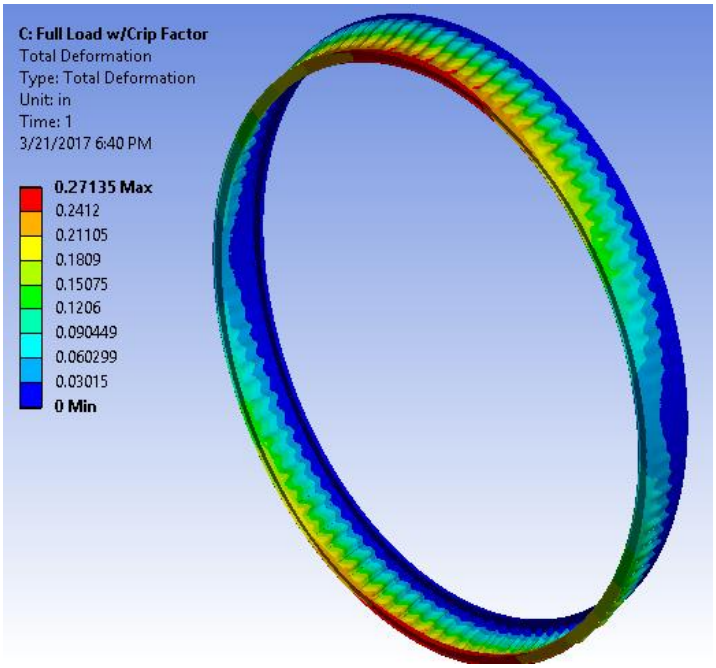

Figure 44. Wide Body: Deformation Analysis with Crippling Factor (Scaled x32)

The total deformation analysis (see Figure 44) shows a maximum deformation of ~0.27-in along the upper and lower sections of the ring. Extrapolating these deflections to the tail of the aircraft, assuming linear deflection at every ring section, results in a total deflection of 1.46-ft.

CONCLUSION

The goal of this analysis is to prove a structural analysis tool, coupled with parametric CAD, can be developed to expedite aircraft development. While improvements to this design method are endless, this analysis proves a structural sizing tool of this nature is possible. From the two cases analyzed in this report, the sizing is within the range of actual aircraft structure, with slight increases in skin thickness. Unfortunately, due to the assumption of fixing the aircraft at the wing spar, the applied loads are larger than typically seen in flight. This ripples into the structural sizing resulting in inherently oversized components. While a more in depth analysis would reduce the sizing requirements, the goal of this tool is to give a solid starting point moving into the preliminary design stage. The FEA analysis confirmed the structure, with the applied crippling factor, is sized correctly in both cases for the applied loads. As previously discussed, implementing a dynamic flight model into the sizing algorithm would eliminate the load discontinuity and improve the sizing accuracy.

While this program is by no means perfect, the analysis proves the method is possible. Adding additional functionality such as cutouts, tapered forward and aft sections, empennage structural sizing, and increased load accuracy, a program of this nature could conceivably size the full fuselage structure. Coupled with a parametric CAD model it provides a visual representation of the conceptual aircraft structure and starting point moving into the preliminary design stage.

REFERENCES

[1]MacNeal, R.H., "Automatic Structural Design Optimization", Lockheed Aircraft Corporation, SN-392, 12 December 1956.

[2]MSC Software Corporation, "Company History," http://www.mscsoftware.com/page/msc-software. [retrieved 10 October 2016]

[3]Schmit, L. A., "Structural Design by Systematic Synthesis," American Society of Civil Engineers, Paper 1960-42, Sept. 1960.

[4]Vanderplaats, G. N., "Automated Optimization Techniques for Aircraft Synthesis" AIAA Paper, Aug. 1976.
[5]Rastogi, N., Ghosh, D. K., Vanderplaats, G. N., "Discrete Optimization Capabilities in Genesis Structural Analysis and Optimization Software," AIAA Paper 2002-5646, Sept. 2002.

[6]Carty, A., "An Approach to Multidisciplinary Design, Analysis & Optimization for Rapid Conceptual Design", AIAA Paper 2002-5438. Sept. 2002.

[7]Carty, A., Davies, C., "Fusion of Aircraft Synthesis and Computer Aided Design", AIAA Paper 2004-4433. Sept. 2004.

[8]Vandenbrande, J. H., Grandline, T. A., Hogan, T., "The search for the perfect body: Shape control for multidisciplinary design optimization", AIAA Paper 2006-928. Jan. 2006.

[9]Ledermann, C., Ermanni, P., Kelm, R., "Dynamic CAD objects for structural optimization in preliminary aircraft design," *Aerospace Science and Technology*. published online 24 Aug. 2006; Vol. 10, 2006, pp. 601-610.

[10]Hahn., A. S., "Vehicle Sketch Pad: A Parametric Geometry Modeler for Conceptual Aircraft Design," AIAA Paper 2010-657. Jan. 2010.

[11]Chaput, A.J., Akay, E., Rizao-Patron, S., "Vehicle Sketch Pad (VSP) Structural Layout Tool," AIAA Paper 2011-357. Jan. 2011.

[12]Beam, S., "Collier Comes Back to His Future at Langley" *NASA* [online], http://www.nasa.gov/centers/langley/news/researchernews/rn_collier.html [retrieved 16 October 2016].

[13]"Our Products" *HyperSizer* [online], http://hypersizer.com/about/ [retrieved 16 October 2016].

[14]Alonso, J.J., Martin, J.R.R.A., Reuther, J.J., Haimes, R., Crawford, C.A., "High-Fidelity Aero-Structural Design Using a Parametric CAD-Based Model," AIAA Paper 2003-3429. Jun. 2003.

[15]Hutchins, C., Missoum, S., Takahashi, T.T., "Fully Parameterized Wing Model for Preliminary Design," AIAA Paper 2010-9120, Sept. 2010.

[16]Takahashi, T.T., Lemonds, T., "Prediction of Wing Structural Mass for Transport Category Aircraft Conceptual Design,"AIAA Paper 2015-3374, 2015.

[17]Niu, M., "Buckling and Stability of Structures," *Airframe Structural Design,* 2nd ed., Hong Kong Conmilit Press LTD, Hong Kong, 2011, pp. 118-161.

[18]Niu, M., "Fuselage," *Airframe Structural Design,* 2nd ed., Hong Kong Conmilit Press LTD, Hong Kong, 2011, pp. 376-429.

[19]MIL-HDBK-5J

[20]14 CFR § 25.303 (2012)

[21]14 CFR § 25.305 (2012)

[22]14 CFR § 25.613 (2012)

[23]"Aviation Maintenance Technician Handbook-Airframe", Federal Aviation Administration, Vol 1, 2012, Chap 4.

[24]Needham, R. A., "The Ultimate Strength of Aluminum-Alloy formed Structural Shapes in Compression", *Journal of the Aeronautical Sciences.* Vol 21, No. 4, 1954, pp. 217-229.

[25]Niu, M., "Fuselage," *Airframe Structural Design,* 2nd ed., Hong Kong Conmilit Press LTD, Hong Kong, 2011, pp. 588-589.

[26]14 CFR § 25.365 (2012)

[27]14 CFR § 25.337 (2012)

[28] "777-200LR / -300ER / -Freighter Airplane Characteristics for Airport Planning", *Boeing Commercial Airplanes* [online], file:///E:/777_2lr3er.pdf [retrieved 21 March 2017].

APPENDIX

DATA COLLECTED IN THE WIDE BODY ANALYSIS

Table 21. Wide Body: Frame Dimensions

Station	Cap Width (in)	Web Height (in)	Thickness (in)
1	0.75	2.00	0.064
2	0.75	2.00	0.064
3	0.75	2.00	0.064
4	0.75	2.00	0.064
5	0.75	2.00	0.064
6	0.75	2.00	0.064
7	0.75	2.00	0.064
8	0.75	2.00	0.064
9	0.75	2.00	0.064
10	0.75	2.00	0.064
11	0.75	2.00	0.064
12	0.75	2.00	0.081
13	0.75	2.00	0.102
14	0.75	2.00	0.102
15	1.00	2.00	0.102
16	1.00	2.50	0.081
17	1.00	2.50	0.102
18	1.00	2.50	0.102
19	1.00	2.50	0.125
20	1.00	2.50	0.125
21	1.25	2.50	0.125
22	1.25	2.50	0.125
23	1.25	3.00	0.102
24	1.25	3.00	0.102
25	1.25	3.00	0.125
26	1.25	3.00	0.125
27	1.25	3.00	0.125
28	1.25	3.00	0.250
29	1.25	3.00	0.250
30	1.25	3.00	0.250
31	1.25	3.00	0.250
32	1.25	3.00	0.250
33	1.25	3.00	0.250
34	1.25	3.00	0.250
35	1.25	3.00	0.250
36	1.25	3.00	0.250
37	1.25	3.00	0.250

38	1.25	3.00	0.250
39	1.25	3.00	0.250
40	1.25	3.00	0.250
41	1.25	3.00	0.250
42	1.50	3.00	0.250
43	1.50	3.00	0.250
44	1.50	3.00	0.250
45	1.50	3.50	0.250
46	1.50	3.50	0.250
47	1.50	3.50	0.250
48	1.50	3.50	0.250
49	1.50	3.50	0.250
50	1.50	3.50	0.250
51	1.50	3.50	0.250
52	1.50	3.50	0.250
53	1.50	3.50	0.250
54	1.50	3.50	0.375
55	1.50	3.50	0.375
56	1.50	3.50	0.375
57	1.50	3.50	0.375
58	1.50	3.50	0.375
59	1.50	3.50	0.375
60	1.75	4.00	0.375
61	1.75	4.00	0.375
62	1.75	4.00	0.375
63	1.75	4.00	0.375
64	1.75	3.50	0.375
65	1.75	3.50	0.375
66	1.75	3.50	0.375
67	1.75	3.50	0.375
68	1.50	3.50	0.375
69	1.50	3.50	0.375
70	1.50	3.50	0.375
71	1.50	3.50	0.375
72	1.50	3.50	0.375
73	1.50	3.50	0.375
74	1.50	3.50	0.375
75	1.50	3.50	0.375
76	1.50	3.50	0.375
77	1.50	3.50	0.375

78	1.50	3.50	0.375
79	1.50	3.50	0.375
80	1.50	3.50	0.375
81	1.50	3.50	0.250
82	1.50	3.50	0.250
83	1.50	3.50	0.250
84	1.50	3.50	0.250
85	1.50	3.50	0.250
86	1.50	3.50	0.250
87	1.50	3.50	0.250
88	1.50	3.50	0.250
89	1.50	3.00	0.250
90	1.50	3.00	0.250
91	1.25	3.00	0.250
92	1.25	3.00	0.250
93	1.25	3.00	0.250
94	1.25	3.00	0.250
95	1.25	3.00	0.250
96	1.25	3.00	0.250
97	1.25	3.00	0.250
98	1.25	3.00	0.250
99	1.25	3.00	0.250
100	1.25	3.00	0.250
101	1.25	3.00	0.250
102	1.25	3.00	0.125
103	1.25	3.00	0.125
104	1.25	3.00	0.102
105	1.25	2.50	0.125
106	1.00	2.50	0.125
107	1.00	2.50	0.125
108	1.00	2.50	0.102
109	1.00	2.50	0.081
110	1.00	2.00	0.102
111	0.75	2.00	0.102
112	0.75	2.00	0.081
113	0.75	2.00	0.064
114	0.75	2.00	0.064
115	0.75	2.00	0.064
116	0.75	2.00	0.064
117	0.75	2.00	0.064

118	0.75	2.00	0.064
119	0.75	2.00	0.064
120	0.75	2.00	0.064
121	0.75	2.00	0.064
122	0.75	2.00	0.064
123	0.75	2.00	0.064
124	0.75	2.00	0.064
125	0.75	2.00	0.064

Table 22. Wide Body: Sample Shear Buildup

Stringer #	Af (in^2)	y (in)	yAf (in^3)	(Y^2)As (in^4)	Σ(yAs) (in^3)	$\bar{q}_{bending}$ (lbf/in)	Fxy (lbf/in^2)	Fxx (lbf/in^2)
1	0.469	122.0	57.2	6976.9				
					57.2	27.86	344.8	44464
2	0.938	121.8	114.2	13906.6				
					171.4	83.49	1033.3	44388
3	0.625	121.2	75.7	9177.1				
					247.1	120.39	1490.0	44163
4	0.625	120.1	75.1	9022.0				
					322.2	156.98	1942.8	43788
5	0.625	118.7	74.2	8807.8				
					396.4	193.13	2390.2	43265
6	0.625	116.9	73.0	8537.3				
					469.4	228.72	2830.7	42596
7	0.625	114.6	71.7	8214.3				
					541.1	263.63	3262.7	41782
8	0.625	112.0	70.0	7843.1				
					611.1	297.74	3684.9	40827
9	0.625	109.0	68.1	7428.8				
					679.2	330.94	4095.8	39734
10	0.625	105.7	66.0	6976.9				
					745.3	363.11	4493.9	38507
11	0.625	101.9	63.7	6493.5				
					809.0	394.15	4878.1	37149
12	0.625	97.9	61.2	5985.2				
					870.1	423.95	5246.9	35665
13	0.625	93.5	58.4	5458.9				
					928.6	452.41	5599.1	34061
14	0.563	88.7	49.9	4429.5				
					978.5	476.73	5900.1	32342
15	0.563	83.7	47.1	3942.7				
					1025.6	499.67	6184.0	30513
16	0.563	78.4	44.1	3459.2				
					1069.7	521.16	6450.0	28581
17	0.500	72.9	36.4	2653.8				
					1106.1	538.91	6669.7	26552
18	0.563	67.0	37.7	2528.1				

					1143.8	557.28	6897.1	24433
19	0.563	61.0	34.3	2093.1				
					1178.1	574.00	7104.0	22232
20	0.563	54.8	30.8	1686.3				
					1208.9	589.01	7289.7	19955
21	0.500	48.3	24.2	1167.5				
					1233.1	600.78	7435.4	17611
22	0.500	41.7	20.9	870.5				
					1253.9	610.94	7561.2	15207
23	0.500	35.0	17.5	612.1				
					1271.4	619.47	7666.7	12752
24	0.500	28.1	14.1	395.8				
					1285.5	626.32	7751.5	10254
25	0.375	21.2	7.9	168.3				
					1293.5	630.19	7799.4	7721
26	0.375	14.2	5.3	75.2				
					1298.8	632.78	7831.4	5162
27	0.250	7.1	1.8	12.6				
					1300.5	633.64	7842.1	2585
28	0.050	0.0	0.0	0.0				
					1300.5	633.64	7842.1	0
			SUM	257,847		MAX	7842.1	44463.6